FFI RAPPORT

EMITTER IDENTIFICATION – STATISTICS OF DIGITALLY I-Q DEMODULATED RADAR PULSES AND EFFECTS OF ENSEMBLE AVERAGING

SKARTLIEN Roar, ØYEHAUG Leiv

FFI/RAPPORT-2004/00406

EMITTER IDENTIFICATION – STATISTICS OF DIGITALLY I-Q DEMODULATED RADAR PULSES AND EFFECTS OF ENSEMBLE AVERAGING

SKARTLIEN Roar, ØYEHAUG Leiv

FFI/RAPPORT-2004/00406

FORSVARETS FORSKNINGSINSTITUTT
Norwegian Defence Research Establishment
P O Box 25, NO-2027 Kjeller, Norway

FORSVARETS FORSKNINGSINSTITUTT(FFI)
Norwegian Defence Research Establishment

P O BOX 25
NO-2027 KJELLER, NORWAY

UNCLASSIFIED

SECURITY CLASSIFICATION OF THIS PAGE
(when data entered)

REPORT DOCUMENTATION PAGE

1) PUBL/REPORT NUMBER	2) SECURITY CLASSIFICATION	3) NUMBER OF PAGES
FFI/RAPPORT-2004/00406	UNCLASSIFIED	41
1a) PROJECT REFERENCE	**2a) DECLASSIFICATION/DOWNGRADING SCHEDULE**	
FFI-II/864/113	-	

4) TITLE

EMITTER IDENTIFICATION – STATISTICS OF DIGITALLY I-Q DEMODULATED RADAR PULSES AND EFFECTS OF ENSEMBLE AVERAGING

5) NAMES OF AUTHOR(S) IN FULL (surname first)

SKARTLIEN Roar, ØYEHAUG Leiv

6) DISTRIBUTION STATEMENT

Approved for public release. Distribution unlimited. (Offentlig tilgjengelig)

7) INDEXING TERMS

IN ENGLISH	IN NORWEGIAN
a) ESM	a) ESM
b) Emitter identification	b) Emitteridentifikasjon
c) I-Q demodulation	c) I-Q-demodulasjon
d) Quantization	d) Kvantisering
e) Ensemble averaging	e) Ensemble-midling

THESAURUS REFERENCE:

8) ABSTRACT

In electronic warfare and surveillance it is of interest to identify radar emitters based on emitted pulse shapes. Recorded pulse data have uncertainties due to emitter and receiver noise, and due to digital sampling and quantization in the receiver system. It is therefore important to quantify these effects through theory and experiment in order to construct "smart" pulse processing algorithms which minimize the uncertainties in estimated pulse shapes. This report forms a theoretical basis for the statistics of ensemble averaged (intra-pulse) radar data. Inspired by a pulse processor we have developed, we consider a signal processing system involving sampling, A/D-conversion (quantization), I-Q demodulation and ensemble averaging. As input to the system, we adopt a simple but representative radar signal model. The analysis is general and directly applicable to project 864 Profil II.

9) DATE	AUTHORIZED BY	POSITION
2004-03-01	This page only Vidar S Andersen	Director

ISBN 82-464-0841-0

UNCLASSIFIED

SECURITY CLASSIFICATION OF THIS PAGE
(when data entered)

CONTENTS

page

APPENDIX

EMITTER IDENTIFICATION – STATISTICS OF DIGITALLY I-Q DEMODULATED RADAR PULSES AND EFFECTS OF ENSEMBLE AVERAGING

1 INTRODUCTION

One of the issues addressed in Project 864 Profil II is radar emitter identification by means of radar pulse shape recognition. Software and hardware developed for this purpose have been well documented (5, 11, 10). It is crucial that our system does not obscure the signal characteristics in order to identify radar emitters. In this report we consider a digital signal processor which samples the incoming radar signal before the signal is decomposed into I and Q signals. The signal processor DIPP (Digital Intermediate frequency Pulse Processor), developed for the Krest and Profil projects (6, 3, 2), is of this type. We study the signal statistics in terms of the number of bits, input signal to noise ratio, and the number of pulses used in ensemble averaging. The goal of the investigation is to optimize the algorithms used for processing the I and Q output data in order to achieve the sufficient accuracy needed for emitter discrimination and identification. We will concentrate on ways to reduce the statistical uncertainties by different means of ensemble averaging.

2 QUANTIZATION IN NOISE: PRINCIPLES AND BENEFICIAL EFFECTS FROM ENSEMBLE AVERAGING

This section gives a brief introduction to the statistics of a quantized noisy signal, and demonstrate that the expectation of the quantization error diminishes with increasing noise, but at the cost of a larger error variance. As the ensemble average approximates the expectation, it follows that the quantization error (in the ensemble average) can be made much smaller than what corresponds to the bit resolution of the system. We will later encounter a similar analysis in conjunction with the I-Q demodulator when we consider a radar signal model.

2.1 Statistics of the quantizer and noise errors

Consider an analog signal $s(t)$ with additive noise,

$$y_i(t) = s(t) + n_i(t),$$

where t is time, and n is random noise. We observe N realizations of y, and the index $i \in [1, .., N]$ denotes one particular realization i (or radar pulse i). We assume that s is repetitive (independent of i), while n varies with i. We assume a general noise distribution function with zero mean and variance σ^2.

The recorded signal is sampled at discrete t_j, yielding

$$y_{i,j} = s_j + n_{i,j}. \tag{2.1}$$

These samples are quantized through a function Q to obtain the sampled and A/D converted digital signal,

$$x_{i,j} = Q(y_{i,j}).$$

We consider the quantization to be uniform, i.e. the separation between any two neighboring quantization levels is Δ. The probability distribution function (pdf) of $x_{i,j}$ is discrete and generally asymmetric even if the pdf of n is continuous and symmetric. We define the error in the quantized signal as

$$e_{i,j} = x_{i,j} - s_j,$$

accounting for both noise and quantization effects [1].

To illuminate the effect of ensemble averaging, we consider the one-bit case for which the quantizer has two levels: $0, 1$. If the input $y_{i,j}$ is larger than $1/2$ the output $x_{i,j}$ will be 1. Otherwise the output is 0. Consider a constant "signal" $s_j = 1/2$. For zero noise the output is always 1, giving an error $e_{i,j} = x_{i,j} - s_j = 1 - 1/2 = 1/2$. If we introduce noise with a symmetric pdf with zero mean, the quantizer output "flips" between 0 and 1 randomly. The *expectation value* of the output is then $1/2$, since we expect an equal number of zeroes and ones on the output. The expectation value of the error is then zero, $E[e_{i,j}] = 0$.

If the input signal s_j is larger than $1/2$, there will be an error such that $E[e_{i,j}] \neq 0$. For Gaussian noise combined with a uniform quantizer with many levels, one can derive the trigonometric series ((1), equation (33))

$$E[e_{i,j}; s_j] = \frac{\Delta}{\pi} \sum_{k=1}^{\infty} \frac{(-1)^k}{k} \exp[-2\pi^2 k^2 (\sigma/\Delta)^2] \sin(2\pi k s_j/\Delta). \tag{2.2}$$

It is easy to see that $E[e_{i,j}; s_j]$ is *reduced* for increasing noise, such that

$$E[e_{i,j}; s_j] \to 0.$$

The reason for this is that for increasing noise, the discrete pdf of $x_{i,j}$ becomes a more accurate representation of the continuous pdf of $y_{i,j}$ (with expectation s_j). The pdf of $y_{i,j}$ gets "broader" and is thus better resolved on the fixed grid defined by the quantizer cells. For zero noise, $E[e_{i,j}; s_j]$ attains the largest values, and becomes a "sawtooth" function of s_j. For intermediate noise, $E[e_{i,j}; s_j]$ is more sinusoidal as function of s_j, since only the first few terms in the series expansion are important. See Figure 2.1.

Along with the expectation value of the error, there will be an error variance. One can also derive the variance in terms of a trigonometric series (see Appendix A). We have

[1] The noise between different samples of the ensemble, $n_{i,j}$ and $n_{k,j}$, is uncorrelated such that the expectation $E[n_{i,j} n_{k,j}] = 0$ for $k \neq i$. We assume that the correlation time is sufficiently small such that the noise between different time-samples, $n_{i,j}$ and $n_{i,k}$, is also uncorrelated, i.e. $E[n_{i,j} n_{i,k}] = 0$ for $k \neq j$. Thus, in general it holds that

$$E[n_{i,j} n_{k,l}] = \sigma^2 \delta_{ik} \delta_{jl},$$

where δ_{pq} is the usual Kronecker delta.

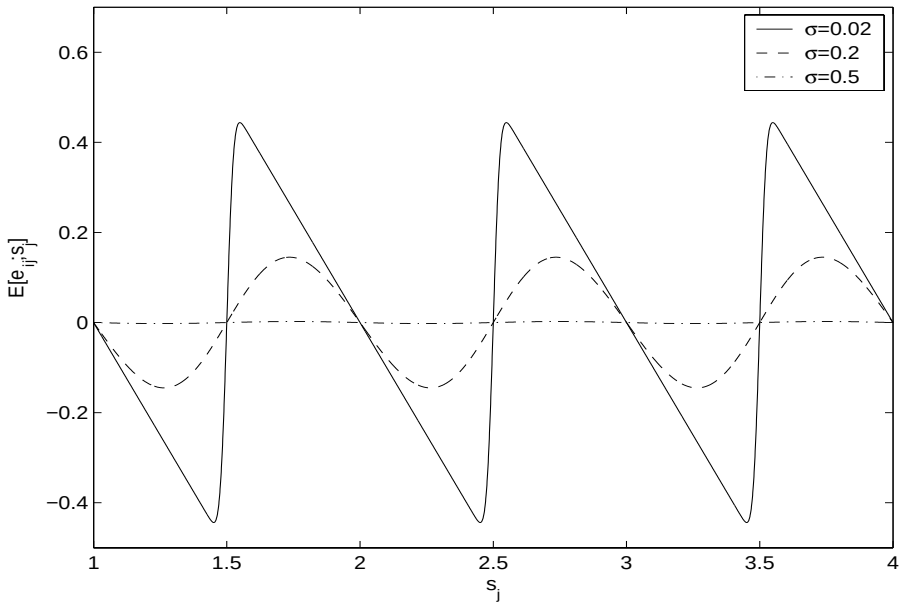

Figure 2.1 *The expected error $E[e_{ij}; s_j]$ as a function of the signal s_j for $\sigma = 0.02$ (solid line), $\sigma = 0.2$ (dashed) and $\sigma = 0.5$ (dashdotted). Here $\Delta = 1$.*

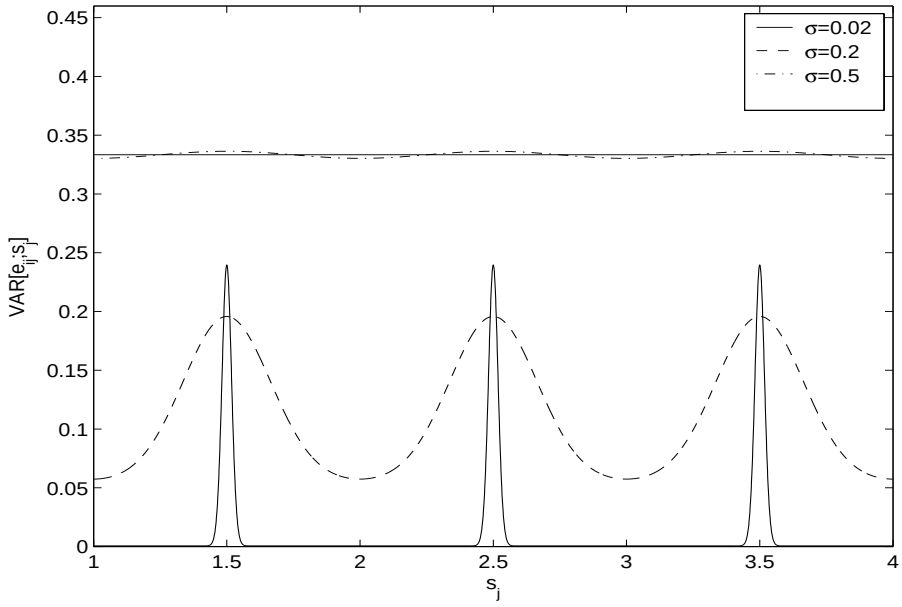

Figure 2.2 *The variance $\mathrm{VAR}[e_{ij}; s_j]$ as a function of the signal s_j for $\sigma = 0.02$ (solid line), $\sigma = 0.2$ (dashed) and $\sigma = 0.5$ (dashdotted). Here $\Delta = 1$. For the case $\sigma = 0.5$ the straight line $\sigma^2 + \Delta^2/12$ is plotted to indicate convergence towards this value with increasing noise.*

$\mathrm{VAR}[e_{i,j};s_j] = E[(e_{i,j})^2;s_j] - E^2[e_{i,j};s_j]$, where $E[e_{i,j};s_j]$ is given in (2.2). For Gaussian noise,

$$E[(e_{i,j})^2;s_j] = \frac{\Delta^2}{12} + \sigma^2 + \frac{\Delta^2}{\pi^2}\sum_{k=1}^{\infty}(-1)^k\left(\frac{1}{k^2} + 4\pi(\sigma/\Delta)^2\right) \times \cos(2k\pi s_j/\Delta)\exp[-2\pi^2(\sigma/\Delta)^2k^2]. \quad (2.3)$$

Combining (2.2) and (2.3) the variance can be calculated. The error variance as a function of s_j is plotted in Figure 2.2 for three values of σ. It is apparent from the exponential factors, that for large noise, $(\sigma/\Delta) \gg 1$,

$$\mathrm{VAR}[e_{i,j};s_j] \to \Delta^2/12 + \sigma^2,$$

such that the error variance becomes *independent* of the signal s_j.

Both a vanishing error expectation, and a variance of σ^2 in the limit, is exactly the property of the analog signal before quantization. We note that since s_j is deterministic,

$$\mathrm{VAR}[x_{i,j};s_j] = \mathrm{VAR}[e_{i,j};s_j] \to \Delta^2/12 + \sigma^2,$$

and

$$E[x_{i,j};s_j] = s_j + E[e_{i,j};s_j] \to s_j.$$

2.2 Ensemble averaging

We will consider the ensemble average of $x_{i,j}$,

$$\bar{x}_j = \frac{1}{N}\sum_{i=1}^{N} x_{i,j}.$$

Ensemble averaging has the desired effect of reducing the variance, as we expect from basic statistics. Using the relations above, one can show that the variance of the ensemble average is

$$\mathrm{VAR}[\bar{x}_j;s_j] = \frac{\mathrm{VAR}[x_{i,j};s_j]}{N} \to \frac{\Delta^2/12 + \sigma^2}{N},$$

where the arrow refers to the large noise limit ($\sigma/\Delta \gg 1$). Thus, the variance of the ensemble average can be made arbitrarily small for increasing ensemble size N. Similarly, in the same limit,

$$E[\bar{x}_j;s_j] = s_j + E[e_{i,j};s_j] \to s_j.$$

It is important to note that the expectation of the ensemble average converges to the input signal s_j for *increasing noise*. Noise is therefore beneficial in this respect, but at the cost of larger variance. A larger variance can of course be compensated by increasing N. It is also important to note that for small noise, the expectation of the ensemble average differs from s_j. Ensemble averaging will not remove this difference, since it originates from the deterministic property of the quantizer and not from the noise.

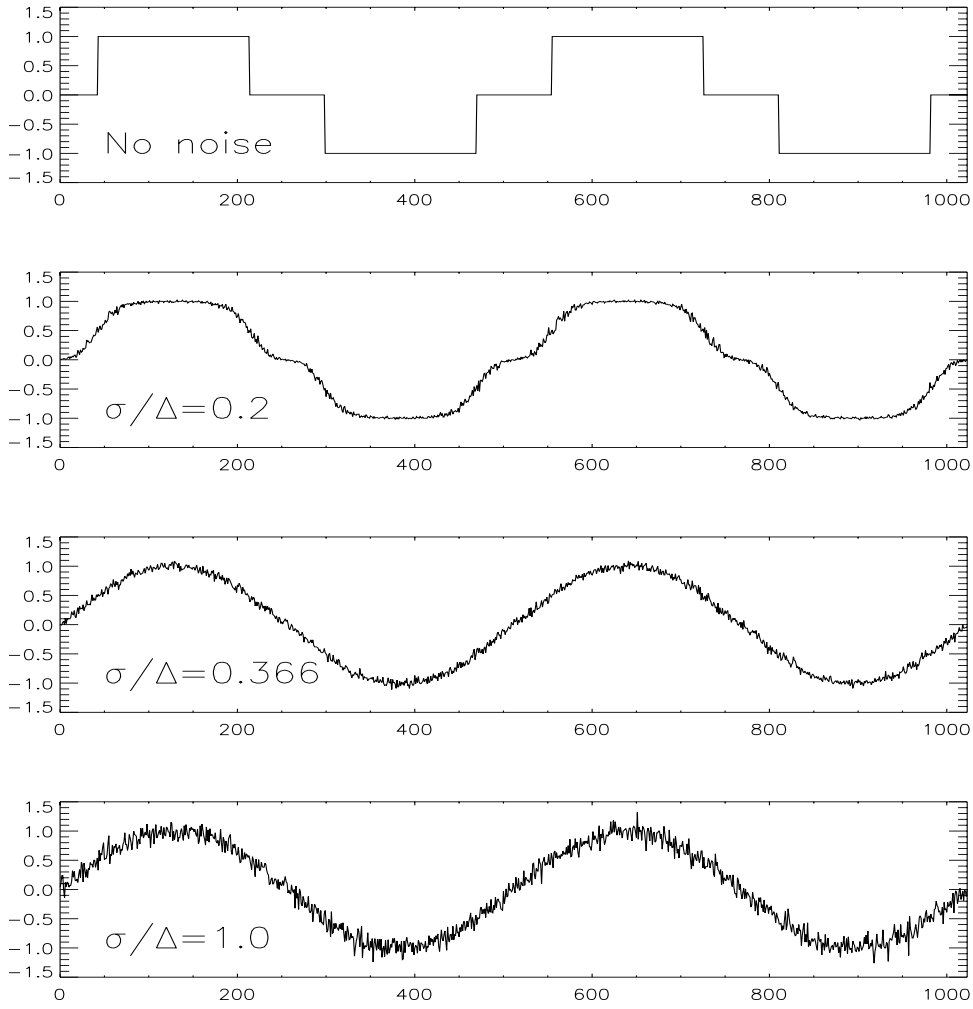

Figure 2.3 An example of the effect of ensemble averaging. A sinusoidal with unit amplitude plus Gaussian noise is quantized by a simple roundoff to the nearest integer. We have performed averaging over an ensemble of $N = 100$ realizations.

We illustrate the effect of noise in Figure 2.3. We have here used
$y_{i,j} = \sin(at_j) + n_i(t_j) = s_j + n_{i,j}$ as an example, where n is Gaussian noise with variance σ^2. We used a simple roundoff to integer numbers as the quantizer function:
$x_{i,j} = Q(y_{i,j}) = \mathrm{Round}(y_{i,j})$, yielding $\Delta = 1$. We have averaged over an ensemble of $N = 100$ realizations. With no noise we obtain a staircase function as expected (upper panel). As the noise increases, the staircase function is smoothed out to resemble the sine-wave s_j, as $E[\bar{x}_j; s_j] \to s_j$. The noise on these curves (or variance) can be reduced to an arbitrarily small level by increasing the ensemble size N.

3 EXPECTATION AND VARIANCE FOR ENSEMBLE AVERAGED I AND Q

We consider a signal processor which treats the incoming signal in the following order: first, the analog raw signal is sampled, then it is quantized (A/D converted) and finally I and Q are calculated by digital mixing and lowpass filtering. These steps represent the DIPP-processor. The

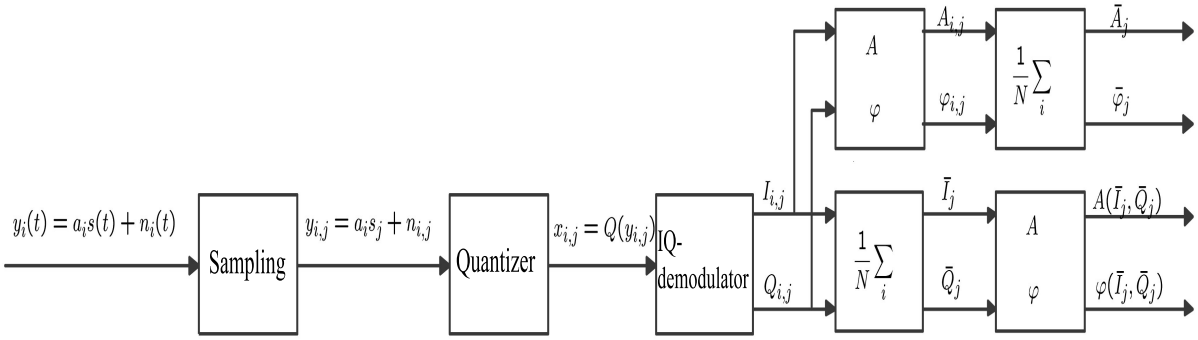

Figure 3.1 *Illustration of the signal processing chain. The analog signal is sampled, quantized and split into I and Q components. These blocks represent the DIPP. The last blocks represent the pulse processing software which extracts amplitude and phase and performs averaging. The details of the I-Q demodulator are given in Figure 3.2.*

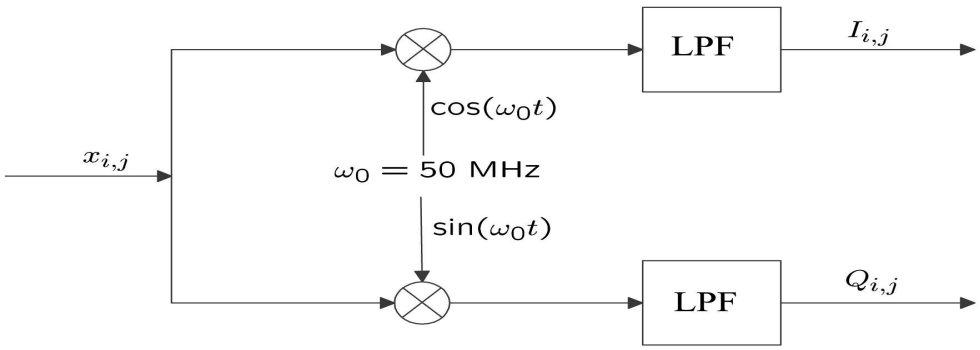

Figure 3.2 *Details of the I-Q demodulator. The digitized (sampled and A/D-converted) signal $x_{i,j}$ is split into I resp. Q by multiplication with a cosine, resp. sine, function and subsequent filtering with a lowpass filter (LPF).*

post-procssing is done in software and consists of calculating amplitude and phase via ensemble averaging over all available radar pulses. The DIPP with post-processing is depicted in Figures 3.1 and 3.2.

Ensemble averaging can be done in two ways; either (i) by computing the average I and Q prior to the computation of amplitude and phase or (ii) by computing amplitude and phase for each pulse followed by averaging. We investigate how the complete system affects the uncertainty and expectation of the output amplitude and phase estimates.

3.1 Signal model

We use a representative model for received radar pulses,

$$y_i(t) = a_i s(t) + n_i(t),$$

where i denotes radar pulse number, $s(t)$ is the repetitive radar pulse, a_i is a scaling which varies with pulse number, and $n_i(t)$ is (non-repetitive) random noise associated to pulse i, with variance

σ^2. We will consider the scaling a_i as a positive random variable ($a_i > 0$) with a distribution $p(a)$ and expectation $E[a] = 1.0$. Without loss of generality, we normalize the model such that the amplitude $A(t)$ of $s(t)$ is of order one during the pulse, and such that σ expresses the noise/signal ratio for $a_i = 1$. With this normalization, $y_i(t)$ is of order one.

The continuous $y_i(t)$ represents the analog signal before sampling. After sampling, we obtain the time-discrete $y_{i,j} = a_i s_j + n_{i,j}$. After A/D conversion (quantization) we obtain $x_{i,j} = Q(y_{i,j})$, which is discrete also in magnitude. This discrete signal is then I-Q demodulated digitally [2].

The functionality of the digital I-Q demodulator is equivalent to the analog version where the input signal is mixed with a local oscillator signal (LO), with subsequent lowpass filtering,

$$\begin{aligned} I_{i,j} &= LPF[x_{i,j}\cos(\omega_0 t_j)] = [x_{i,j}\cos(\omega_0 t_j)] \oplus h_j, \\ Q_{i,j} &= LPF[x_{i,j}\sin(\omega_0 t_j)] = [x_{i,j}\sin(\omega_0 t_j)] \oplus h_j. \end{aligned}$$

Here, ω_0 is the LO-frequency, and $\oplus$ denotes convolution with the impulse response h_j of the lowpass filter. We now consider ensemble averaging of I and Q, and treat only I hereafter, since Q follows a similar calculation. We have now two choices for ensemble averaging I and Q. The first one is a straight ensemble average,

$$\bar{I}_j = \frac{1}{N}\sum_i I_{i,j}.$$

The second one involves normalization,

$$\bar{I}_j = \frac{1}{N}\sum_i \frac{I_{i,j}}{a_i}, \tag{3.1}$$

where we we have estimated the scaling a_i from averaging the amplitude $\sqrt{(I_{i,j})^2 + (Q_{i,j})^2}$ over a suitable interval in j. We obtain

$$\bar{I}_j = [\bar{x}_j \cos(\omega_0 t_j)] \oplus h_j,$$

where

$$\bar{x}_j = \frac{1}{N}\sum_i x_{i,j}$$

in the first case, and

$$\bar{x}_j = \frac{1}{N}\sum_i \frac{x_{i,j}}{a_i},$$

when we use normalization. By invoking the central limit theorem for the sum of random variables, we note that $\bar{I}_j$ (for fixed j) has a pdf which is approximately Gaussian due to the weighted sum of the convolution. For a large ensemble, $\bar{x}_j$ is also close to Gaussian distributed since the ensemble average is also a sum of random variables.

[2] We note that with the given normalization, the quantizer cell size Δ is less than unity to resolve the signal.

3.1.1 Expectation and variance

The goal is to find expressions for the expectation and variance for I (and Q). Obviously,

$$E[\bar{I}_j] = [E[\bar{x}_j; s_j]\cos(\omega_0 t_j)] \oplus h_j.$$

The fluctuating part of $\bar{I}_j$ is

$$\bar{I}_j - E[\bar{I}_j] = [(\bar{x}_j - E[\bar{x}_j; s_j])\cos(\omega_0 t_j)] \oplus h_j,$$

where $\delta\bar{x}_j = \bar{x}_j - E[\bar{x}_j; s_j]$ is the fluctuation in the ensemble average of the quantizer output. We show in Appendix D that the variance is

$$\mathrm{VAR}[\bar{I}_j] = E[(\bar{I}_j - E[\bar{I}_j])^2] = [E[(\delta\bar{x}_j)^2]\cos^2(\omega_0 t_j)] \oplus h_j^2.$$

It is very convenient to rewrite this as

$$\mathrm{VAR}[\bar{I}_j] = [\frac{1}{2}E[(\delta\bar{x}_j)^2](1 + \cos(2\omega_0 t_j))] \oplus h_j^2.$$

The cosine-term shows that $E[(\delta\bar{x}_j)^2]$ is mixed with two times the LO frequency and filtered with the squared impulse response h_j^2. These expressions are general and exact, based on the initial model. We now specialize to the two cases of ensemble averaging, and to the large noise limit $\sigma/\Delta \gg 1$.

3.1.2 Simple averaging

We show in Appendix C.1 that for increasing noise,

$$E[\bar{x}_j; s_j] \to E[a_i]s_j = s_j,$$

since $E[a_i] = 1$. The expectation does indeed reflect the exact I-signal of s, $I_j(s_j)$, as desired,

$$E[\bar{I}_j] = E[a_i][s_j\cos(\omega_0 t_j)] \oplus h_j = I_j(s_j).$$

In the same limit, we show that

$$E[(\delta\bar{x}_j)^2] \to \frac{[\Delta^2/12 + \sigma^2] + s_j^2\mathrm{VAR}[a]}{N}.$$

With constant scaling, $\mathrm{VAR}[a] = 0$, and we may return to the result shown in Section 2.2. It is undesirable that the variance is quadratic in the signal s_j. By inserting $s_j = A(t_j)\sin(\omega_r t_j)$, we obtain, in the large noise limit,

$$\mathrm{VAR}[\bar{I}_j] \to \frac{[\Delta^2/12 + \sigma^2]}{2N}(2\omega_c/\omega_s) + \frac{\mathrm{VAR}[a]}{N}F[s_j^2] \tag{3.2}$$

where $F[s_j^2]$ is due to s_j^2 in $E[(\delta\bar{x}_j)^2]$. We note that $2\omega_c/\omega_s$ comes from the relation

$$2\omega_c/\omega_s = \int_{-\infty}^{+\infty} h^2(t)dt,$$

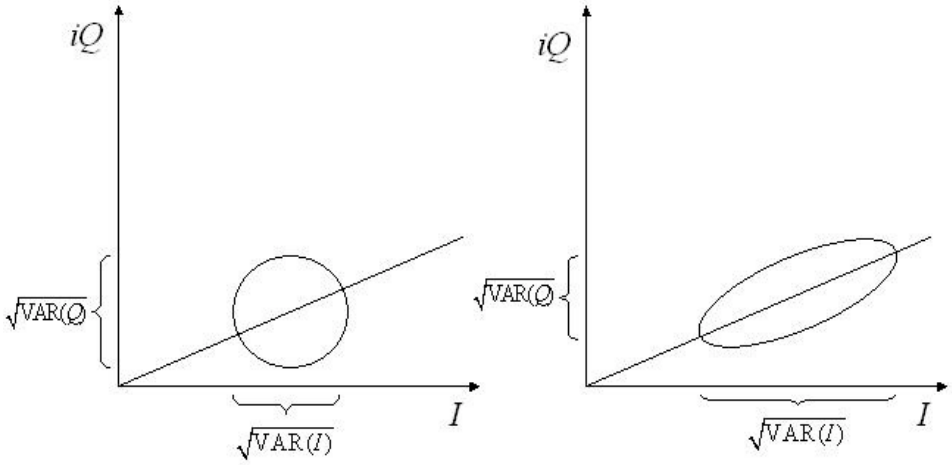

Figure 3.3 For normalized averaging (left panel), the joint probability distribution is symmetric in the complex plane (the I-Q plane), while it is elongated for simple averaging (right panel) due to the different realizations of the scaling a_i. The elongated distribution results in oscillating variances as the phase evolves throughout the pulse. For simple averaging, the variances are the same, $\mathrm{VAR}[\bar{I}_j] = \mathrm{VAR}[\bar{Q}_j]$, and constant with respect to phase.

where we have assumed an ideal filter with $|H(\omega)| = 1$ in the passband. The sampling frequency is ω_s. The integral over the squared filter is simply proportional to the cutoff frequency ω_c.

One can show that $F[s_j^2] > 0$, since the convolution producing this term is always between two positive definite quantities. Outside the radar pulse, $s_j = 0$, and $F[s_j^2] = 0$ such that the variance is a minimum (and constant). Inside the pulse $F[s_j^2] > 0$ varies with time (or j). The significance of the result is that the variance of $\bar{I}_j$ (and $\bar{Q}_j$) is generally dependent on the input signal. Normalized averaging yields in contrast a constant variance also inside the pulse as we shall see in the next section.

Figure 3.3 explains qualitatively why the variance oscillates for simple averaging and is constant for normalized averaging. For simple averaging (left panel), the probability distribution is symmetric in the complex plane (the I-Q plane), while it is elongated for simple averaging (right panel) due to the different realizations of the scaling a_i. The angle between the line through the center of the distributions and the I-axis is the phase of the pulse at a certain time. As the phase changes with time, the variances for the simple averaging oscillate with twice the frequency of I (or Q).

3.1.3 Normalized averaging

We show in Appendix C.2 that for increasing noise,

$E[\bar{x}_j; s_j] \to s_j$.

The expectation is again the exact I-signal of s,

$E[\bar{I}_j] = [s_j \cos(\omega_0 t_j)] \oplus h_j = I_j(s_j)$.

In the same limit, we also show that

$$E[(\delta\bar{x}_j)^2] \to \frac{[\Delta^2/12+\sigma^2]\int_{-\infty}^{+\infty} p(a)/a^2 da}{N}.$$

We note that the quadratic term in s_j has vanished, but we have introduced the expectation of $1/a^2$ as a scaling factor instead. Since now the variance is independent of s, we easily obtain, in the large noise limit,

$$\mathrm{VAR}[\bar{I}_j] \to \frac{[\Delta^2/12+\sigma^2]\int_{-\infty}^{+\infty} p(a)/a^2 da}{2N}(2\omega_c/\omega_s) \equiv (\sigma_I^2/N)\int_{-\infty}^{+\infty} p(a)/a^2 da, \tag{3.3}$$

where we assume that the lowpass filter corresponding to h_j^2 removes the component modulated with $\cos(2\omega_0 t_j)$.

For a uniform distribution $p(a)$ with support in $[1-w, 1+w]$ (noting that $E[a]=1$), $\int_{-\infty}^{+\infty} p(a)/a^2 da = 1/(1-w^2) > 1$. Thus, the factor due to the integral is larger than unity. Therefore, the variance of normalized averaging is larger than the *minimum* variance of the simple average.

3.2 Numerical test

We adopt a uniform distribution $p(a)$ with $E[a]=1$ and support in $[1-w, 1+w]$. We choose $w=\sqrt{1/2}$, and get $\mathrm{VAR}[a] = (2w)^2/12 = 1/6$ and $\int_{-\infty}^{+\infty} p(a)/a^2 da = 1/(1-w^2) = 2$. The noise/cell size ratio is set to $\sigma/\Delta = 2.0$ with $\Delta = 1/8$ and $\sigma = 1/4$. The LO frequency is $\omega_0 = 0.25\omega_s$ (or half the Nyquist frequency). We use $s_j = A(t_j)\sin(\omega_r t_j)$ with carrier frequency $\omega_r = 0.24\omega_s$, giving a relatively small difference frequency $\omega_0 - \omega_r$ for $I(s_j)$. The lowpass filter cutoff is approximately $\omega_c/\omega_s = 0.25$.

We calculated N realizations of I and Q, i.e., $I_{1,j}..I_{2,j}...I_{N,j}$, with accompanying realizations of the noise and the scaling. Figure 3.4 shows simple and normalized ensemble averages of I for $N=100$ (thin lines). The thick line shows $I(s_j)$, and we see that both methods give ensemble averages which converge to the correct value, $I(s_j)$.

The standard deviations $\sqrt{\mathrm{VAR}[I_j]}$ for the two averaging methods are shown in Figure 3.5 (labeled "normalized" and "simple"). The thick solid and dashed lines are the analytical results. The thin curves show the numerical estimate of the standard deviation taken over 1024 realizations of the signal. We see that the theory for the variances agrees very well with the numerical result.

We have $\sigma_I = \sqrt{[\Delta^2/12+\sigma^2](\omega_c/\omega_s)} = 0.125$ for our choice of parameters. This is the minimum standard deviation for simple averaging (as seen outside the pulse), and is given by the first term in 3.2. Inside the pulse, we have an oscillating standard deviation with twice the frequency of $I(s)$. The variance $\mathrm{VAR}[Q_j]$, is shifted half a period inside the pulse, relative to $\mathrm{VAR}[I_j]$ (not plotted).

For normalized averaging, we obtain $\sqrt{\mathrm{VAR}[I_j]} \simeq \sqrt{2}\times 0.125 = 0.175$ from the theory (3.3), and $\mathrm{VAR}[\bar{I}_j] = \mathrm{VAR}[\bar{Q}_j]$. The random fluctuations in the ensemble averages in Figure 3.4 reflect the standard deviation plotted in Figure 3.5, but scaled with $1/\sqrt{N}$ (0.1 in our case).

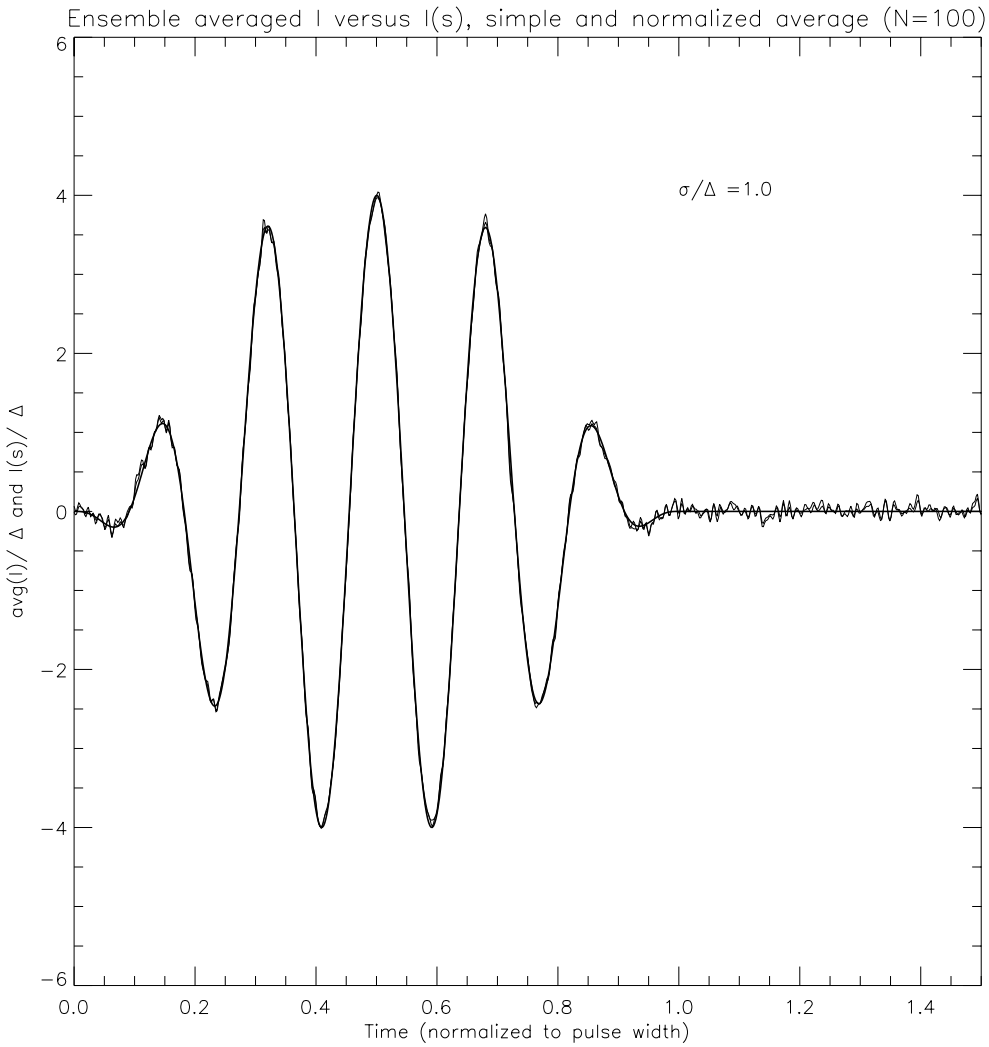

Figure 3.4 Simple and normalized ensemble averages $\bar{I}_j$ for $N = 100$ (thin lines). The thick line shows $I(s_j)$. We see that both ensemble averages coincide with $I(s_j)$. The random fluctuations on the thin curves reflect the variance.

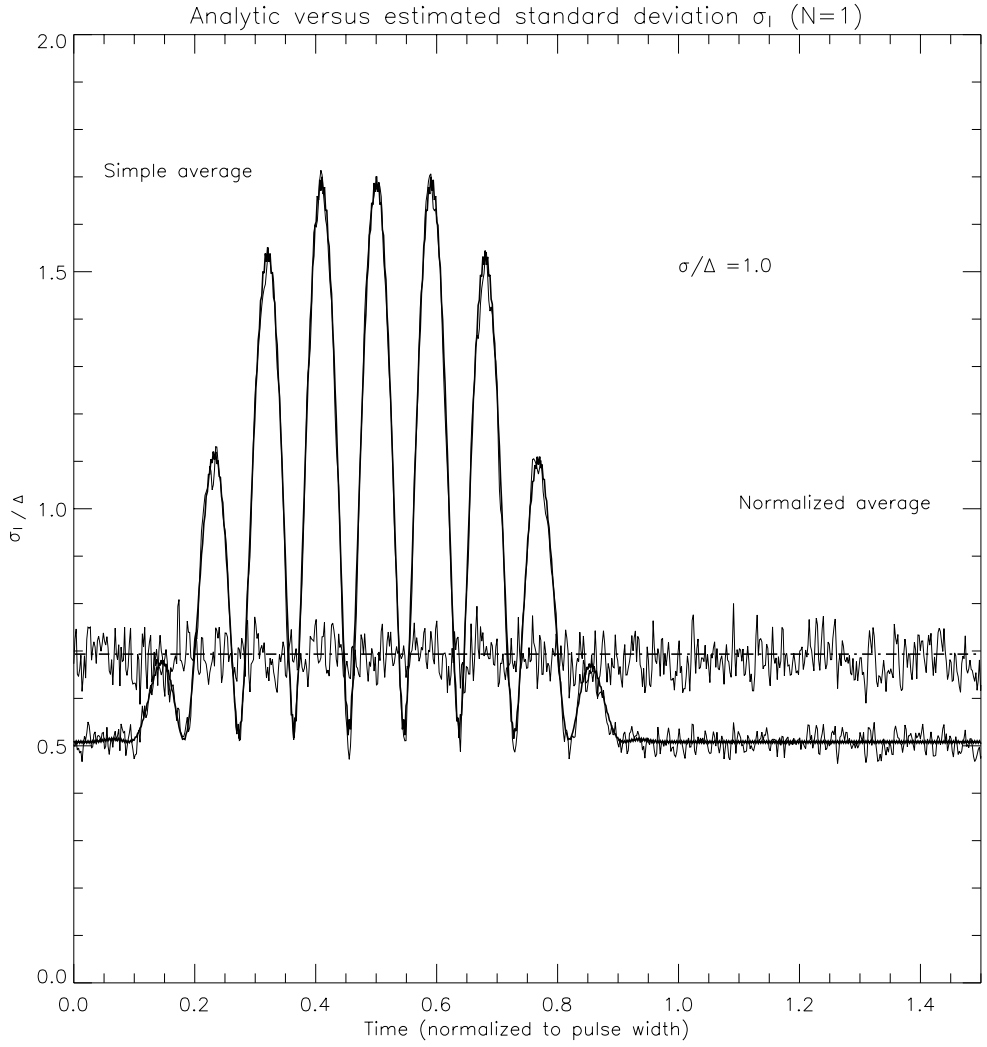

Figure 3.5 *Standard deviation* $\sqrt{\mathrm{VAR}[I_j]}$ *(given by* $N = 1$ *in the general expressions). The thick solid line is the analytical result for simple averaging, and the thick dashed line is the analytical result for normalized averaging. The thin curves show the numerical estimate of the standard deviation taken over* 1024 *realizations of the signal.*

4 PHASE AND AMPLITUDE UNCERTAINTIES (VARIANCES)

Ensemble averaging reduces the uncertainties in both signal amplitude and phase. This section addresses how the averaging should be performed in order to minimize the uncertainty.

There were two ways of handling I and Q before post-processing: A) we normalize I and Q with the amplitude scaling a, or B) we use I and Q as they are. We noted that the variances after normalization were lower than the mean variance within the un-normalized pulse (Figure 3.5). For this reason, it seems that normalization is the best choice and *we will therefore only discuss normalization hereafter*.

There are two different ways of generating the phase and the amplitude: **Method I** refers to calculating phase and amplitude of ensemble averaged I/a and Q/a. **Method II** refers to calculating phase and the amplitude of each individual realization of the pair $(I/a, Q/a)$, before ensemble averaging [3]. In radar-terms, Method I can be regarded as "coherent integration" and Method II as "incoherent integration", where "integration" is to be understood as ensemble averaging.

4.1 Phase and amplitude of ensemble averaged I and Q (Method I)

For sufficiently large ensemble N (say, $N > 10$), we have noted that the corresponding averages $\bar{I}$ and $\bar{Q}$ (3.1) tend to normal distributions (Gaussian random variables) by invoking the Central Limit Theorem from basic statistics. For normalized averaging, the joint distribution of $\bar{I}$ and $\bar{Q}$ is also symmetric. One can then immediately use the classical "Rician" probability distributions for the amplitude and the phase which applies to Gaussian and symmetric joint distributions. Appendix E gives a discussion of these distributions in their asymptotic limits.

4.1.1 Amplitude distribution

Let $A_0 \equiv \sqrt{(E[I_j])^2 + (E[Q_j])^2}$ be the amplitude corresponding to the expectation values (we have shown that $E[I_j] = I(s_j)$ and $E[Q_j] = Q(s_j)$ in the regime $\sigma/\Delta \gg 1$). The pdf of the amplitude $A_j = \sqrt{(I_j)^2 + (Q_j)^2}$ is Rician ((7), page 498) for each time sample j,

$$p(A; A_0, \sigma^2_{I,N}) = A/\sigma^2_{I,N} e^{-(A^2+A_0^2)/2\sigma^2_{I,N}} I_0(AA_0/\sigma^2_{I,N}), \tag{4.1}$$

where I_0 is the modified Bessel function of zero order. In our case,

$$\begin{aligned} \sigma^2_{I,N} &= (\sigma^2_I/N) \int_{-\infty}^{+\infty} p(a)/a^2 da \\ \sigma^2_I &= (\omega_c/\omega_s)[\Delta^2/12 + \sigma^2], \end{aligned} \tag{4.2}$$

corresponding to (3.3).

[3] We note that normalization does not matter for the phase, since $\mathrm{Arg}(I/a + iQ/a) = \mathrm{Arg}(I + iQ)$.

4.1.2 Phase distribution

The pdf of the phase, $\phi = \mathrm{Arg}(I_j + iQ_j)$, is $p(\phi - E[\phi]; q)$, where (page 501 in (7) and page 167 in (4)),

$$p(\phi; q_N) = \frac{e^{-q_N}}{2\pi} + \frac{\sqrt{q_N}\cos(\phi)e^{-q_N \sin^2(\phi)}}{\sqrt{4\pi}}\left[1 + 2\mathrm{Erf}(\sqrt{2q_N}\cos(\phi))\right], \quad q_N = \frac{A_0^2}{2\sigma_{I,N}^2}, \tag{4.3}$$

where Erf denotes the usual error function; $\mathrm{Erf}(x) = (1/\sqrt{2\pi})\int_0^x e^{-t^2/2}\,dt$. Due to symmetry properties in the complex plane, the expectation of the phase $E[\phi]$ is independent of A_0 and is equal to that of the input signal s:

$E[\phi] = \mathrm{Arg}(E[I_j] + iE[Q_j]) = \mathrm{Arg}(I(s) + iQ(s))$.

It is important to note that the variance of the phase, $\mathrm{VAR}[\phi]$, is dependent only on the square of the signal to noise ratio via $q_N = A_0^2/2\sigma_{I,N}^2$, where $\sigma_{I,N}$ is given in (4.2).

4.2 Ensemble averaged phase and amplitude (Method II)

We now calculate the phase and the amplitude of each individual realization of the pair $(I/a, Q/a)$, before ensemble averaging. One can show that the joint distribution $p(I/a, Q/a)$ is *non-Gaussian*. This can be handled by treating the Rician distributions as conditional distributions for given a, and then integrating over $p(a)$ to obtain the non-Rician amplitude and phase distributions. The resulting variances can then be calculated numerically. The variances for the ensemble averaged quantities are then obtained by scaling with $1/N$, by the assumption of uncorrelated realizations.

4.2.1 Amplitude distribution

For given a, I/a and Q/a are Gaussian random variables with equal variances, σ_I^2/a^2. The corresponding expected amplitude is A_0. The marginal Rician distribution is then obtained by inserting the fixed A_0, and the variance σ_I^2/a^2. On integrating over $p(a)$ we obtain the amplitude distribution,

$$p(A; A_0, \sigma_I^2) = \int_0^\infty a^2(A/\sigma_I^2)e^{-a^2(A^2+A_0^2)/2\sigma_I^2} I_0(a^2 A A_0/\sigma_I^2)p(a)da, \tag{4.4}$$

where σ_I is given in (4.2).

4.2.2 Phase distribution

For the phase, we make a similar substitution, $q \to a^2 q$, and obtain

$$\begin{aligned} p(\phi; q) &= \int_0^\infty \left[\frac{e^{-a^2 q}}{2\pi} + \frac{\sqrt{a^2 q}\cos(\phi)e^{-a^2 q \sin^2(\phi)}}{\sqrt{4\pi}}\left[1 + 2\mathrm{Erf}(\sqrt{2a^2 q}\cos(\phi))\right]\right] p(a)da, \\ q &= \frac{A_0^2}{2\sigma_I^2}, \end{aligned} \tag{4.5}$$

where, again, σ_I^2 is given in (4.2). We note that normalization does not matter for the phase calculation for the pair $(I/a, Q/a)$, such that the expression above is valid also for the un-normalized case.

4.3 Large signal to noise ratio

4.3.1 Phase variance

The phase variance for both methods tend to the same value for $A_0 \gg \sigma_I$. In this limit $a^2 q \gg 1$ (for not too small a), such that the integrand of (4.5) for Method II can be replaced by (E.3) of Appendix E. The resulting phase variance is

$$\sigma^2_{\phi,M2} = \frac{1}{2qN} \int_{-\infty}^{+\infty} p(a)/a^2 da = (1/N)(\sigma_I^2/A_0^2) \int_{-\infty}^{+\infty} p(a)/a^2 da. \tag{4.6}$$

Similarly, the phase distribution (4.3) for Method I has the variance $1/(2q_N)$ in the same limit, and it follows that $\sigma^2_{\phi,M2} = \sigma^2_{\phi,M1}$. We conclude that the two methods give different phase variance only for moderate signal to noise ratios, which means a low amplitude radar pulse, or on the rising and falling edges of the pulse in general.

4.3.2 Amplitude variance

Also the amplitude variance for both methods tend to the same value for $A_0 \gg \sigma_I$. In this limit, the amplitude distribution tends to a Gaussian near A_0. The integrand of (4.4) is then a Gaussian with expectation $E[A; a] = A_0 + (\sigma_I^2/a)^2/(2A_0)$. One can then show that

$$\sigma^2_{A,M2} = (\sigma_I^2/N) \left\{ \int_{-\infty}^{+\infty} p(a)/a^2 da + \mathcal{O}(\sigma_I^2/A_0^2) \right\}.$$

Similarly, the amplitude distribution (4.1) for Method I has variance $\sigma^2_{I,N}$, in the same limit. It then follows that $\sigma^2_{A,M2} \to \sigma^2_{A,M1}$ for $A_0/\sigma_I \to \infty$. We conclude that the two methods give different amplitude variances only for moderate signal to noise ratios.

4.4 Comparison of the methods

We ask: *Which of the two methods leads to the smallest amplitude and phase variance for moderate signal to noise ratios?* The answer to the above question is non-trivial, since the computation of amplitude and phase is nonlinear.

We need to express how the variances depend on the noise, the signal amplitude and N. With $\sigma^2_{I,N}$ in the amplitude and phase pdfs (4.1) and (4.3), we obtain for Method I:

$\sigma^2_{A,M1}(A_0, [\sigma_I^2/A_0^2]/N)$

for the amplitude, and

$\sigma^2_{\phi,M1}([\sigma_I^2/A_0^2]/N)$

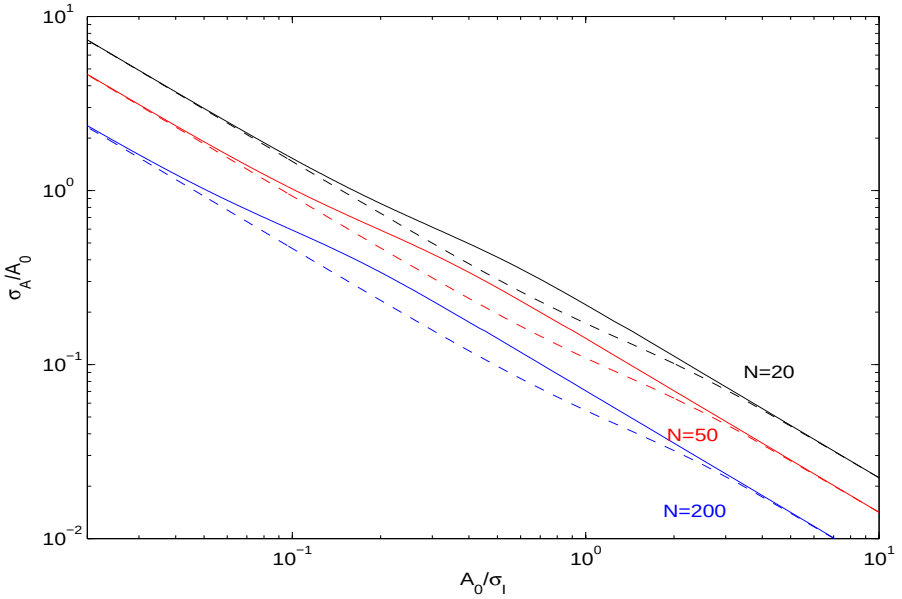

Figure 4.1 *Output NSR as function of input SNR, A_0/σ_I, when $A_0 = 0.1$ for Method I (solid line) and Method II (dashed line) with $N = 20$ (blue), $N = 50$ (green) and $N = 200$ (red).*

for the phase.

For Method II, we can assume that the terms in the averaging sum are uncorrelated, and obtain the usual $1/N$-law,

$$\sigma^2_{A,M2}(A_0, [\sigma_I^2/A_0^2])/N$$

for the amplitude, and

$$\sigma^2_{\phi,M2}([\sigma_I^2/A_0^2])/N$$

for the phase. The difference between the methods then arises when we scale the argument with N, in contrast to scaling the variances with N. Either way, it is trivial to note that the amplitude as well as the phase variance decrease with increasing N.

Comparing the performance of Methods I and II then comes down to establishing which is the smallest of the functions $f_{M1}(x/N)$ and $f_{M2}(x)/N$, where $x = (\sigma_I/A_0)^2$ and the f's express the phase variance or the amplitude variance. Thus, given the value of N we should be able to establish for which signal-to-noise ratios Method I is favorable over Method II and vice versa. One can expect that the differences between the variances of Method I and II vary as function of N and σ_I in general. Below, we quantify these differences.

In the following we choose the half width of $p(a)$ equal to $w = 0.7$. For given signal strength and noise level, we find the variances by integrating over the pdf's, when an explicit form is not available.

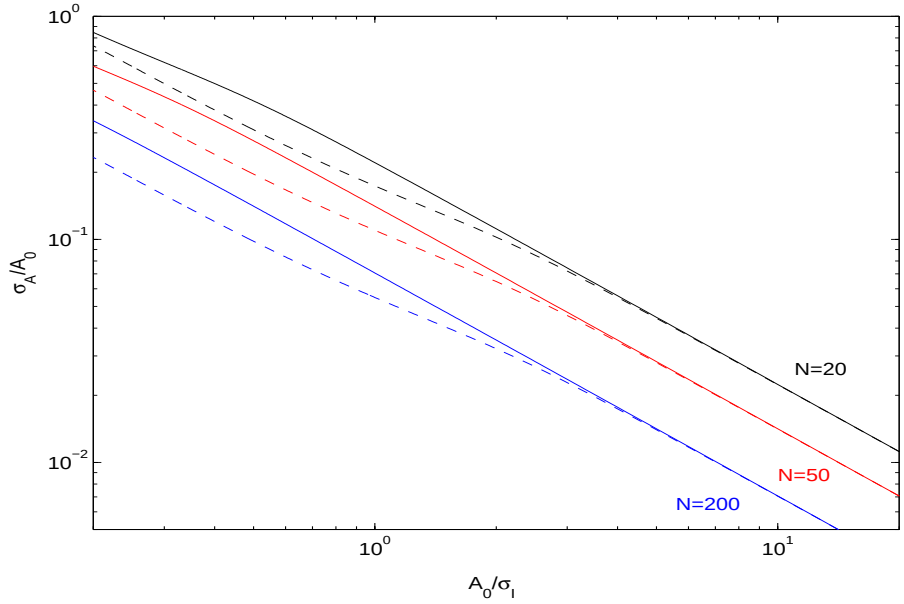

Figure 4.2 *Output NSR as function of input SNR, A_0/σ_I, when $A_0 = 1$ for Method I (solid line) and Method II (dashed line) with $N = 20$ (blue), $N = 50$ (green) and $N = 200$ (red).*

4.4.1 Method I vs Method II for amplitude

There are two independent parameters in the amplitude pdf; A_0 and σ_I. Figures 4.1 and 4.2 illustrate how the output noise to signal (NSR) ratio σ_A/A_0 relates to the input signal to noise (SNR) ratio A_0/σ_I for $A_0 = 0.1$ and $A_0 = 1$, respectively, for $N = 20, 50, 200$. Method I is shown with a full line and Method II with a dashed line.

From Figure 4.1 it is evident that at very low input SNR there is very little difference between the two methods for all the chosen N. For high input SNR we also expect equal variances as discussed previously. This is also seen in Figure 4.2 where the variances for the two methods coalesce near SNR=10. Both figures display the same tendency regarding medium input SNR, namely that Method II is the best (Method II has lower output NSR than Method I).

We also plot the output NSR as function of N for several choices of the input SNR. The cases for $A_0 = 0.1$ and $A_0 = 1$ are plotted in Figures 4.3 and 4.4, respectively. We reach the same conclusion, namely that Method II is the best choice.

4.4.2 Method I vs Method II for phase

The variance of the phase depends only on the input SNR via $q = A_0^2/\sigma_I^2/2$. Figure 4.5 displays the standard deviation of the phase (measured in degrees) for several values of N as a function of input SNR. For poor input SNR less than about 2, Method II is the best. For input SNR>2, Method I is the best. The two methods have indistinguishable variances for input SNR larger than about 20. This is also expected from the previous analysis.

In Figure 4.6, the standard deviation of the phase is plotted against the number of realizations N

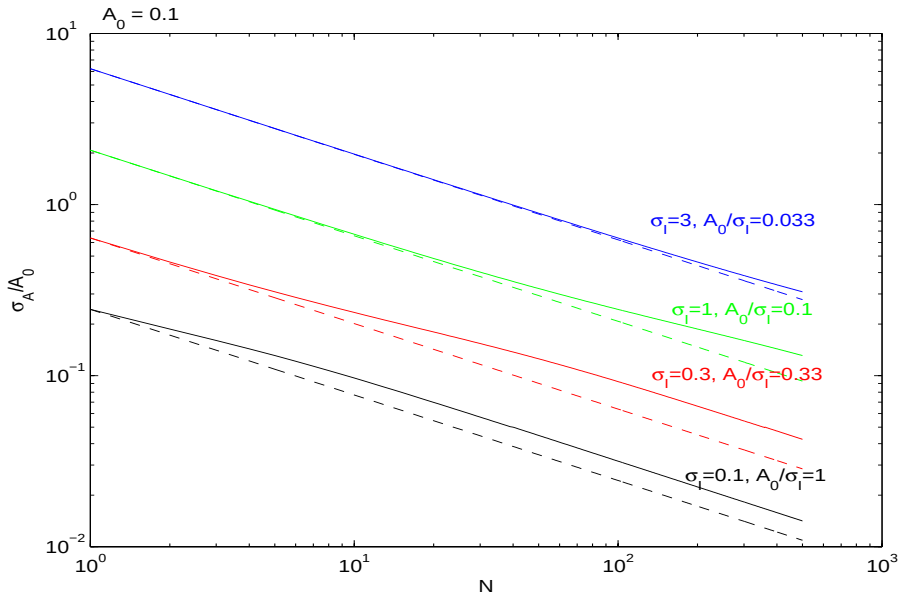

Figure 4.3 *Output NSR, σ_A/A_0, with $A_0 = 0.1$ as a function of the input SNR A_0/σ_I, for Method I (solid line) and Method II (dashed line). The parameters are $\sigma_I = 0.2$ (blue), $\sigma_I = 1$ (green), $\sigma_I = 3$ (red) and $\sigma_I = 10$ (black).*

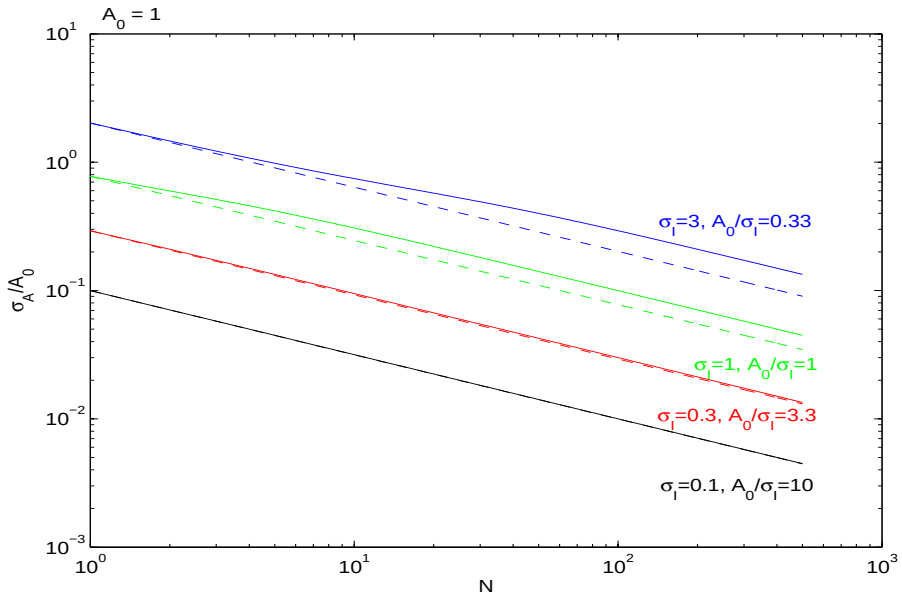

Figure 4.4 *Output NSR, σ_A/A_0, with $A_0 = 1$ as a function of the input SNR σ_I, for Method I (solid line) and Method II (dashed). The parameters are $\sigma_I = 0.2$ (blue), $\sigma_I = 1$ (green), $\sigma_I = 3$ (red) and $\sigma_I = 10$ (black).*

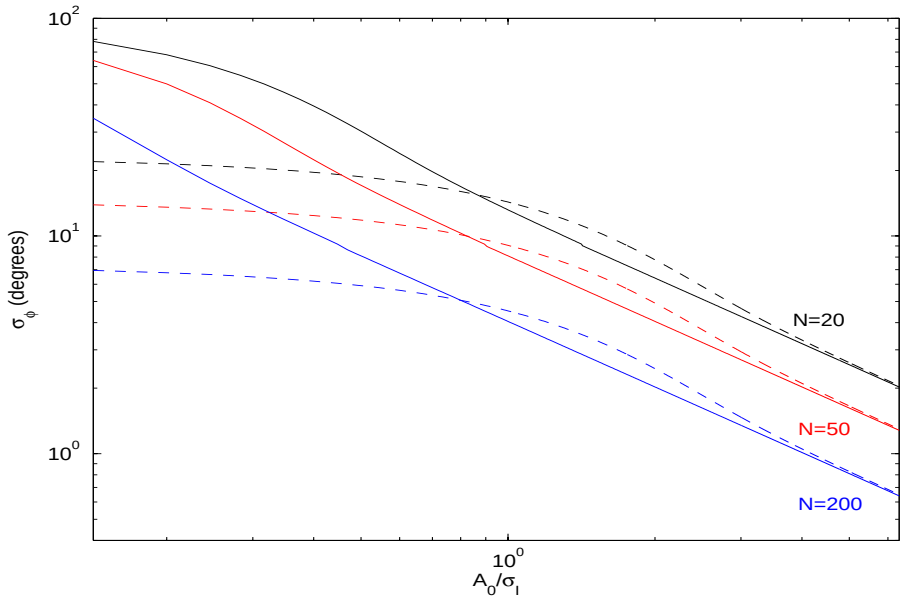

Figure 4.5 *The phase standard deviation measured in degrees for Method I (solid line) and Method II (dashed) as function of input SNR A_0/σ_I with the number of realizations chosen as $N = 20$ (blue), $N = 50$ (green) and $N = 200$ (red).*

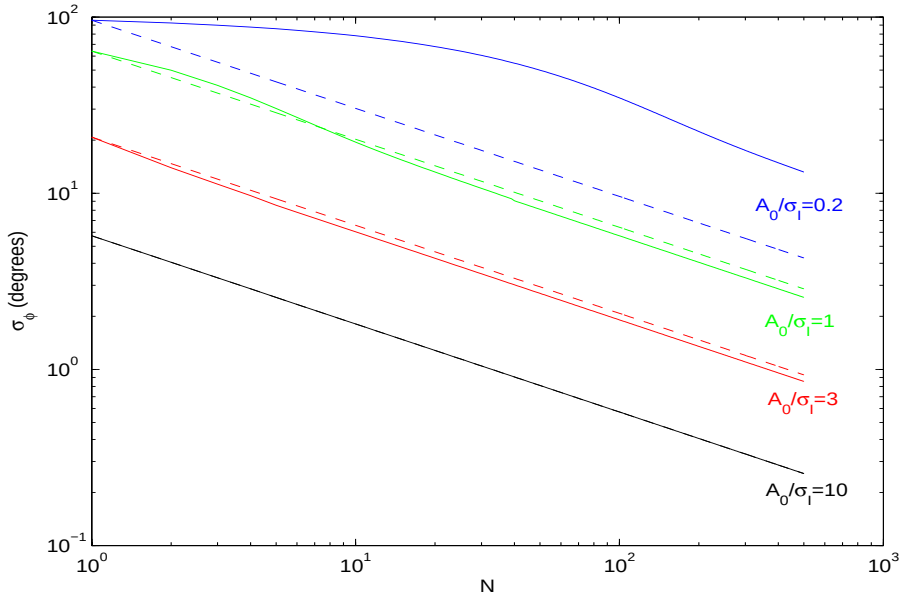

Figure 4.6 *The phase standard deviation as function of N, for Method I (solid line) and Method II (dashed) with parameter values $A_0/\sigma_I = 0.2$ (blue), $A_0/\sigma_I = 1$ (green), $A_0/\sigma_I = 3$ (red) and $A_0/\sigma_I = 10$ (black).*

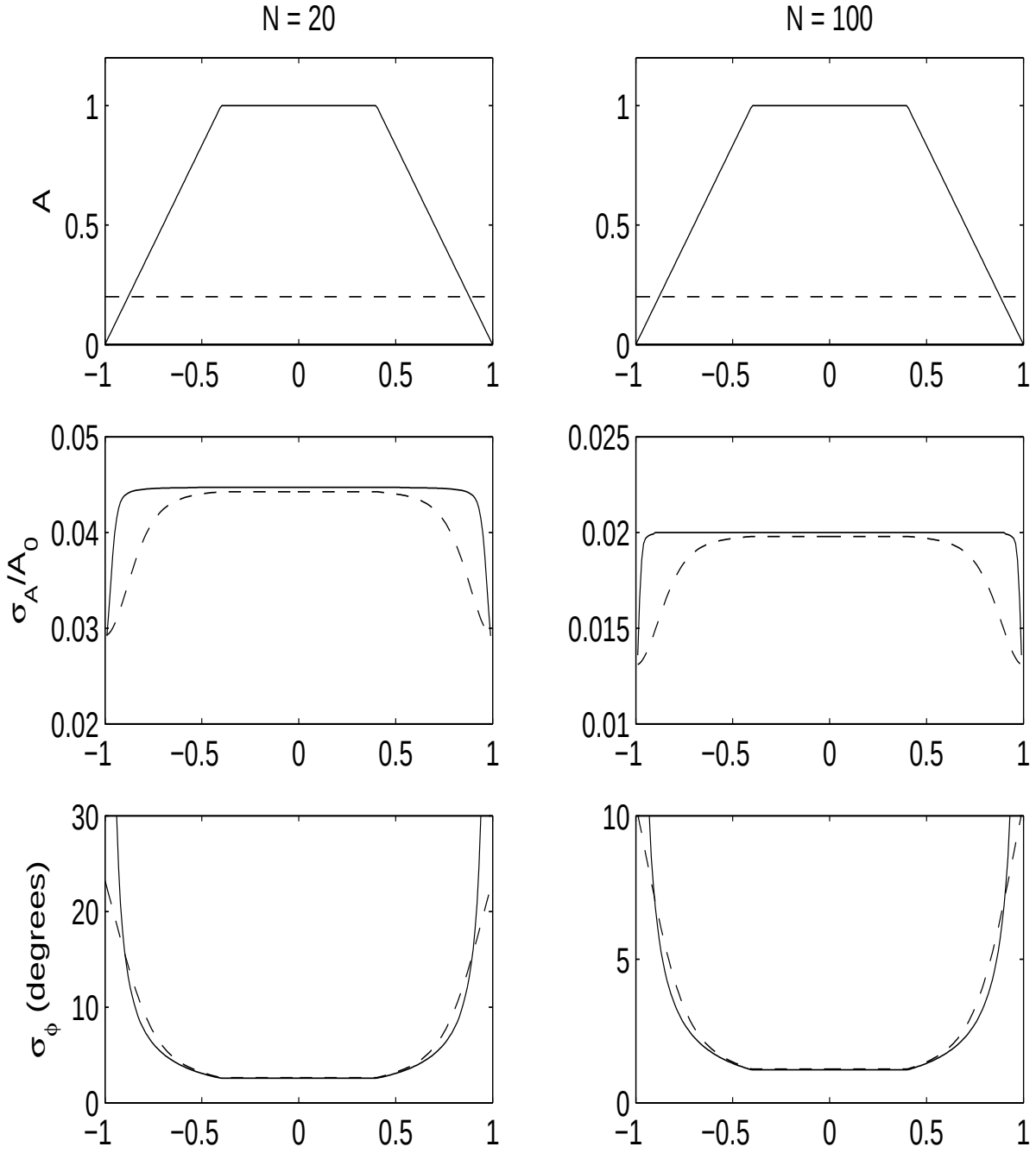

Figure 4.7 Amplitude of an artificial radar pulse (top panel, left and right are equal). The (time dependent) noise to signal ratio σ_A/A_0 for Method I (solid line) and Method II (dashed) is shown for $N = 20$ (middle panel, left) and $N = 100$ (middle panel, right). In the lower panel the (time dependent) standard deviation of the phase, σ_ϕ, is shown. Method I (solid line) and Method II (dashed line).

for several values of the input SNR (A_0/σ_I). Again, for poor input signal-to-noise ratios (illustrated by SNR=1 and SNR=0.2), Method II is the best. Method I is the best for the larger input SNR's (3 and 10). The difference between the two methods converges rapidly to zero with increasing input SNR.

Finally, we illustrate the results in Figure 4.7 with an artificial radar pulse. The top panels show the pulse amplitude (solid line) and the noise standard deviation σ_I (dashed line). The signal to noise ratio (input SNR) is about 5 when the pulse reaches unity amplitude. We note that the SNR varies throughout the pulse. The two columns are for $N = 20$ and $N = 100$. For the amplitude, we conclude again that Method II is favorable, regardless of the input SNR. For this example, we find about 25-30 % difference between the standard deviations on the rising and falling edges, and about 5 % within the pulse. For the phase, we conclude that Method I is favorable when the SNR is relatively large, and that Method II is favorable when the SNR is poor (we note that poor SNR occurs in general on rising and falling edges of an otherwise strong pulse). The figure shows about 15 % difference between the standard deviations within the pulse and about 80 % difference leading and trailing edges of the pulse.

5 A NOTE ON PROCESSING WITH AN INTEGER I-Q DEMODULATOR WITH A FIR-FILTER

For numerical purposes, it is an advantage to implement integer I-Q demodulators. The FIR-filter is integer valued and operates on (quantized) integer signals. We have

$$I_{i,j} = LPF[\cos(\omega_0 t_j)x_{i,j}] = \cos(\omega_0 t_j)x_{i,j} \oplus H_j,$$

where

$$H_j = \mathrm{Round}(h_j),$$

and equivalently for $Q_{i,j}$. The LO frequency is chosen as one quarter the sampling frequency, $\omega_0 = 2\pi(f_s/4)$, $\omega_0 t_j = \omega_0(j/f_s) = j(\pi/2)$, such that $\cos(\omega_0 t_j)$ is integer, i.e. on the form $[..., -1, 0, 1, 0, ...]$, and similarly for $\sin(\omega_0 t_j)$. We conclude that all samples of I and Q are integer multiples of Δ;

$$I_{i,j}, Q_{i,j} \in [... - n\Delta, ..., -\Delta, 0, +\Delta, ..., +n\Delta...].$$

For x integer, Δ=1, such that I and Q are also integers. We note that the roundoff of the impulse response introduces a (deterministic) modification of the filter response, and has no consequence for stability or accuracy for the filtered signal.

An important effect in the context of stability comes from the finite length of the FIR-filter which display ripples in the frequency response. Many radars transmit signals with various carrier frequencies. Altered carrier frequency will then alter the filter characteristics in the bandwidth of the signal, and change the shape of the filtered radar pulse.

Figure 5.1 exemplifies the effect from filter ripples on the pulse shape. The amplitude of an artificial radar pulse with zero noise is depicted for three values of the carrier frequency, $f_0 = 0$,$f_0 = 10$ and $f_0 = 21$. The amplitude spectrum of the signals are plotted over the filter

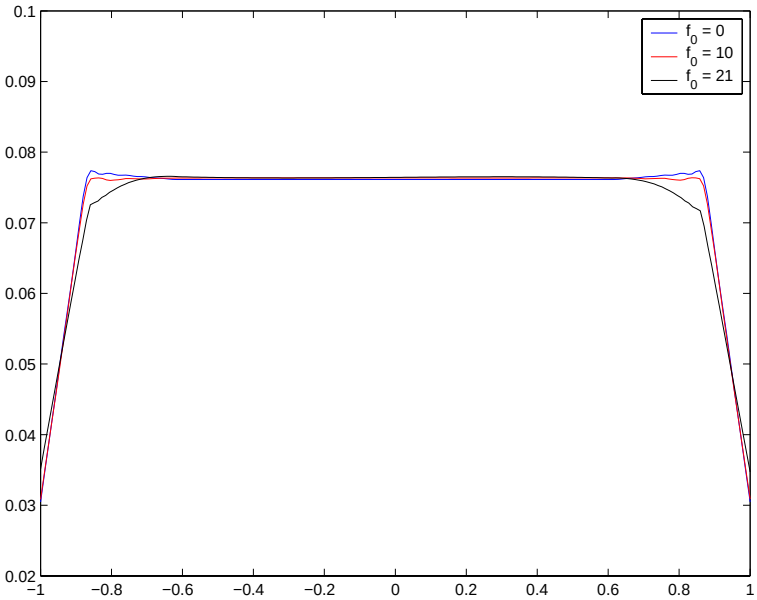

Figure 5.1 *Amplitude of an artificial radar pulse with carrier frequencies $f_0 = 0$ (blue), $f_0 = 10$ (red) and $f_0 = 21$ (black).*

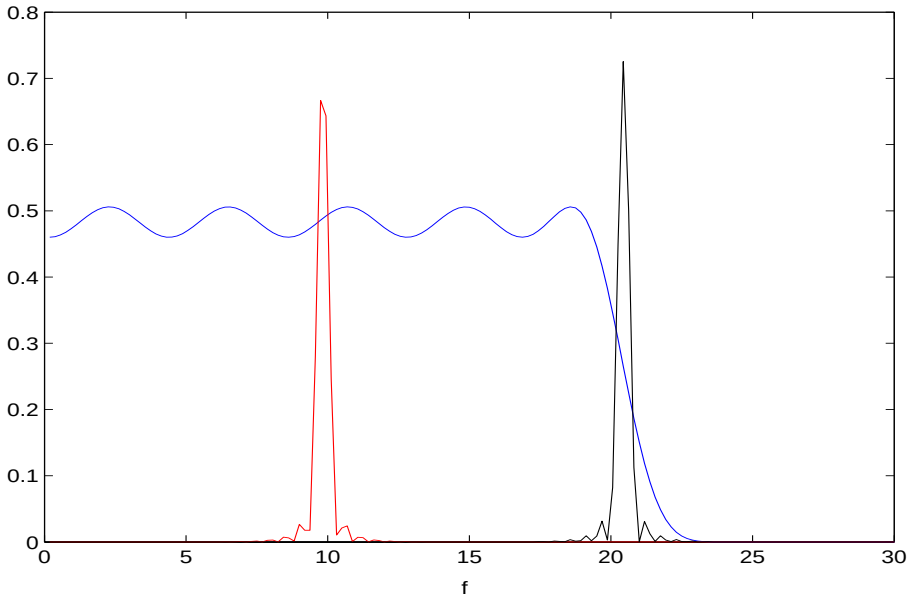

Figure 5.2 *Spectrum of the radar pulse with carrier frequencies $f_0 = 10$ (red) and $f_0 = 21$ (black) plotted with the low-pass filter (LPF in Figure 3.2). Note that the spectrum of the signal with $f_0 = 21$ lies on the trailing edge of the filter.*

response in Figure 5.2, and we see that the two lowest frequencies represent the filter passband, while the highest frequency represents the the edge of the filter. Given these deterministic filter effects, the analysis proceeds as in the preceding sections, but with a $I(s_j)$ which is dependent on carrier frequency.

6 DISCUSSION

Some potentially important effects were not included in our analysis. These are uncertainty in the time sampling (the pulses are sampled at varying time lags determined by the trigger threshold and thermal noise), uncertainty in estimated scaling a, multi-path effects (8) and uncertainties due to pulse-to-pulse phase offset. We will discuss phase offset and time sampling uncertainty below, and propose a way to further reduce the uncertainty by elimination of an optimal number of low amplitude pulses.

When we perform averaging on I and Q in Method I, we need to estimate the phase offset for each pulse. This introduces extra uncertainty which we have not accounted for in the analysis. In particular, one may then in the end come to the conclusion that Method II is better for the phase than Method I, since Method II does not depend on the phase offset in the same manner.

To further elaborate on phase calculation via Method II, we note that the phase corresponding to $(I_{i,j}, Q_{i,j})$ can be expressed as

$$\phi_{i,j} = \Delta\phi_j + \omega_i t_j + \theta_i + \delta\phi_{i,j},$$

where $\Delta\phi_j$ corresponds to the expected frequency modulation of the pulse, $\omega_i t_j$ corresponds to the carrier frequency, with a possible pulse dependent frequency ω_i, θ_i is the phase offset which varies from pulse to pulse, and $\delta\phi_{i,j}$ is the phase noise which is distributed according to (4.5). By averaging (Method II), we obtain an ensemble average with expectation $\Delta\phi_j + E[\omega_i]t_j + \theta_i$. One may now estimate the linear part $E[\omega_i]t_j + \theta_i$ from the averaged $\phi_{i,j}$ and subtract in order to obtain the modulation or "fingerprint" $\Delta\phi_j$. In order to avoid the extra uncertainty associated with the estimation of the linear part, one should choose a representation in the form of coefficients where the linear part affects only one of these coefficients. This coefficient can then be discarded.

Time sampling uncertainty manifests itself as an extra noise contribution with non-zero correlation length – if the pulse is approximately linear over the sampling interval Δt, the extra noise has a distribution of the same form as the time lag probability distribution, and with a standard deviation proportional to the signal slope. Since the radar pulse represents an oscillating signal, we can imagine that the total noise variance can be time-dependent. Possible fluctuations in the emitted pulse (stochastic deviations from the expectation) can probably also be regarded as extra noise with non-zero correlation length.

For moderately large signal to noise ratios, we showed that both methods have variances that are proportional to the integral

$$\frac{\int_{-\infty}^{+\infty} p(a)/a^2 da}{N}.$$

An interesting possibility is to discard data for which $a < a_0$ (a_0 is a threshold to be determined), to minimize the variances. Let N_{tot} be the available number of pulses. If we eliminate those

pulses for which $a < a_0$, we obtain a new distribution $p(a; a_0)$. The integral above may be rewritten as

$$R(a_0) = \frac{\int_{-\infty}^{+\infty} p(a; a_0)/a^2 da}{N_{\text{tot}} \int_{a_0}^{+\infty} p(a)/a^2 da}.$$

One can now see the possibility of minimizing R (and therefore the variances) by finding an optimal threshold a_0. In an operative situation, $p(a)$ is determined by the actual data-set.

We have shown that bit-resolution (the number of bits for a given signal range) is not the only crucial parameter for obtaining accuracy. First, one can minimize the effect of quantization error in the ensemble averages, if the input noise is *larger* than the quantizer step-size ($\sigma/\Delta > 1$). In the large noise limit, the expectation value of I and Q corresponds to the noise-free analog signal, and the variances are approximately equal to the variances of the analog I and Q. Second, the uncertainties in the phase and amplitude estimates can be reduced to an arbitrary low level by ensemble averaging of a larger number of pulses. For coarser bit resolution (larger Δ), and with the requirement $\Delta < \sigma$, we need a larger number of pulses N to average over to obtain the same accuracy. Thus, high resolution A/D converters are not necessarily needed when N is large enough. For given σ and Δ, the lower limit on N can only be determined by first obtaining the required accuracy needed to distinguish the emitter pulse forms.

We did not discuss the probability distributions in the context of un-normalized I and Q although we argued that the amplitude variances for both methods are generally larger than for normalized I and Q. We also showed that the phase variance for Method II is the same whether we normalize or not. By numerical experiments we have observed that the phase variance for Method I (without normalization) is similar to the normalized case. We may then, for Method I and phase calculation, choose not to normalize I and Q before averaging.

We discussed only a uniform scaling distribution $p(a)$, with a certain half-width of $w = 0.7$. We have also tested the procedures for $w = 0.0$ (constant a), and arrived at similar conclusions. It is therefore unlikely that a different form of $p(a)$ (say Rayleigh distribution) will alter the conclusions dramatically.

7 CONCLUSIONS

This report forms a theoretical basis for the statistics of ensemble averaged (intra-pulse) radar data. Quantization errors were accounted for in the context of a digital I-Q demodulator. The results are directly applicable to project 864 Profil II, as an aid in constructing "smart" pulse processing algorithms which minimize the uncertainties in estimated pulse shapes.

Based on experience with recorded radar data, we adopted a signal model including a repetitive radar pulse s scaled randomly in amplitude with the parameter a, and including additive noise with given variance σ^2. We have investigated two methods: I) normalized averaging for I and Q with subsequent calculation of amplitude and phase, and II) averaging of phase and amplitude from samples of normalized I and Q. The normalization consists of dividing the signal with estimates of the scaling parameter a.

The uncertainty in the phase and amplitude estimates depends on the choice of method, the the number of radar pulses N to average over, and the average signal to noise ratio $(E[a]s)/\sigma$. The

following question was asked: *Which method gives the smallest uncertainty in the amplitude and phase estimates?* Both methods give the same variances for large signal to noise ratios (greater than 10). For smaller SNR, we find significant differences between the variances especially at leading and trailing edges of the pulse.

We find that Method II is better than Method I for amplitude regardless of the input SNR and N. We gave an example using a radar-pulse with moderate SNR of 5. The example showed about 25-30 % difference in standard deviations (uncertainties) on the rising and falling edges of the pulse, and about 5 % difference within the pulse. For phase, we find that Method I is better than Method II for moderate SNR, regardless of N. The example showed about 15 % difference between the standard deviations within the pulse. For very small signal to noise ratios, we conclude that Method II is the best also for the phase, regardless of N. Here, the example gave about 80 % difference on leading and trailing edges of the pulse.

The uncertainties diminish roughly as $1/\sqrt{N}$ for both methods, such that when the standard deviation is reduced to one half by choice of method, we need only $N/4$ radar pulses to average over to obtain the same accuracy. Thus, choosing the best method is important in the context of processing speed. If processing speed is of no concern due to otherwise fast algorithms and equipment, we note that any of the methods can be sufficient by simply increasing the number of radar pulses N to average over. We have also shown that bit-resolution is not the only crucial parameter for obtaining accuracy when we perform ensemble averaging – lower bit-resolution can be compensated by larger N in general.

APPENDIX

A A NOTE ON THE FIRST AND SECOND MOMENTS OF THE ERROR

Omitting subscripts, $y = s + n$, $x = Q(y)$, and $E[y] = s$. The expectation (given s) of the moments of the error $e = x - s$ can be found by using the discrete $p(x; s)$. Alternatively, one can write $e = [Q(y) - y] + [y - E[y]]$, where the first bracket is the quantization error for a given y, and the second bracket is the deviation from the average y. Thus, one can obtain the mean error by using $p(y; s)$ in the following way,

$$E[e; s] = \int dyp(y; s)([Q(y) - y] + [y - E[y]]) = \int dyp(y; s)[Q(y) - y].$$

Carbone and Petri (1) use the Fourier series for $q(y) \equiv [Q(y) - y]$ to obtain $E[e; s]$ in terms of the characteristic function Φ of $p(y; s)$. This comes about due to the weighting by trigonometrical terms (in the Fourier series) when integrating over y. We note that s is arbitrary.

Using $\delta y \equiv y - E[y]$, we obtain for the second moment

$$E[e^2; s] = \int dyp(y; s)(q + \delta y)^2 = \int dyp(y; s)(q^2 + 2q\delta y + \delta y^2).$$

By using the Fourier series for q, we obtain

$$E[q^2; s] = \frac{\Delta^2}{12} + \frac{\Delta^2}{\pi^2} \sum_{k=1}^{\infty} \frac{(-1)^k}{k^2} \mathrm{Re}[\Phi(k/\Delta) \exp[i2k\pi(s/\Delta)].$$

For the cross term, one cannot easily express the result in terms of the characteristic function, as we see from the general expression

$$2E[q\delta y; s] = 2\frac{\Delta}{\pi} \int_{-\infty}^{+\infty} dyp(y - s) \sum_{k=1}^{\infty} (-1)^k (y - s) \sin(2k\pi(y/\Delta)).$$

For Gaussian noise, we get

$$2E[q\delta y; s] = 4\sigma^2 \sum_{k=1}^{\infty} (-1)^k \cos(2k\pi(s/\Delta)) \exp[-2\pi^2(\sigma/\Delta)^2 k^2].$$

Finally,

$$E[\delta y^2] = \sigma^2,$$

which is simply the noise variance. We get

$$\begin{aligned} E[(e_{i,j})^2; s] &= E[q^2; s] + 2E[q\delta y; s] + E[\delta y^2] \\ &= \frac{\Delta^2}{12} + \sigma^2 + \frac{\Delta^2}{\pi^2} \sum_{k=1}^{\infty} (-1)^k \left(\frac{1}{k^2} + 4\pi(\sigma/\Delta)^2 \right) \times \\ &\quad \cos(2k\pi(s/\Delta)) \exp[-2\pi^2(\sigma/\Delta)^2 k^2] \end{aligned}$$

for Gaussian noise. This procedure becomes more complex for higher moments, and one might consider the first approach using the discrete $p(x; s)$. Finally we note that
$\mathrm{VAR}[x_{i,j}; s] = E[(\delta e_{i,j})^2; s] = E[(e_{i,j})^2; s] - E^2[e_{i,j}; s]$ since $\delta e_{i,j} = e_{i,j} - E[e_{i,j}; s]$.

B MEAN SQUARE ERROR AND OPTIMAL NOISE

The mean square error over M samples of the ensemble averaged signal is defined as

$$\mathrm{MSE}(\sigma, N) = \frac{1}{M}\sum_{j=1}^{M} E[(\bar{x}_j - s_j)^2].$$

This quantity measures the deviation from the signal s in a global sense, and accounts for both the expectation of the error $e_{i,j} = \bar{x}_{i,j} - s_j$ and the variance of the error. Since the expected error diminishes and the variance increases for growing noise, we may expect a minimum point for the mean square error as function of the variance of the noise, σ. One can show (see (9)) that the mean square error can be expressed in variances and expectations;

$$\mathrm{MSE}(\sigma, N) = \frac{1}{M}\sum_{j=1}^{M} [\frac{\mathrm{VAR}[x_{i,j}; s_j]}{N} + (E[e_{i,j}; s_j])^2].$$

The first contribution, $\mathrm{VAR}[x_{i,j}; s_j]/N$, is the variance of the quantized signal, divided by the number of realizations the averaging is performed over, and $E[e_{i,j}; s_j]$ is the expectation value of the error.

For large noise, $\sigma \gg \Delta$, $E[e_{i,j}; s_j]$ can be neglected and $\mathrm{VAR}[x_{i,j}; s_j] \simeq \Delta^2/12 + \sigma^2$ regardless of the signal level s_j, as noted above. This situation gives a mean square error

$$\mathrm{MSE}(\sigma, N) \simeq (\Delta^2/12 + \sigma^2)/N.$$

For small noise, the variance can be neglected, and the contribution from the error $E[e_{i,j}; s_j]$ dominates. One can show that $\mathrm{MSE}(0, N) = \Delta^2/12$ for a linear s (or sufficiently small Δ). In (9) we proved that there is an optimum noise level where the MSE is minimum, for arbitrary noise pdf's. For Gaussian noise, we found the relation

$$\sigma_{\mathrm{opt}}/\Delta = \frac{1}{2\pi}\sqrt{\ln[2(N-1)]}.$$

The optimum noise level $\sigma_{\mathrm{opt}}/\Delta = 0.366$ for $N = 100$ is demonstrated in Figure 2.3.

C VARIANCE AND EXPECTATION OF THE QUANTIZED, AND THE QUANTIZED AND SCALED SIGNAL

We remind the reader that the quantized signal is $x_{i,j} = Q(a_i s_j + n_{i,j})$. The goal is to find, for fixed time index j, the expectation and variance of the quantized signal, $x_{i,j}$, and for the quantized and scaled signal $x_{i,j}/a_i$. We will in the following suppress the subscripts i and j, for clarity.

C.1 Simple average

We define the conditional probability distribution $p(x; as)$ as the probability density of x given the scaling a. The total pdf of x is then

$$p(x; s) = \int_{-\infty}^{+\infty} p(a)p(x; as)da,$$

where $p(a)$ is the pdf of the scaling a. The expectation

$$E[x;s] = \int_{-\infty}^{+\infty} xp(x;s)dx = \int_{-\infty}^{+\infty} p(a)E[x;as]da$$

is simply the average of the conditional expected value $E[x;as]$ (given a). According to the initial considerations for increasing noise, we conclude that $E[x;as] \to as$ such that $E[x;s] \to E[a]s$.

With

$$x - E[x;s] = (x - E[x;as]) + (E[x;as] - E[x;s]) \equiv \delta x + \Delta E(x;as),$$

the variance is generally

$$\begin{aligned}
\mathrm{VAR}[x;s] &= \int_{-\infty}^{+\infty} (x - E[x;s])^2 p(x;s)dx \\
&= \int_{-\infty}^{+\infty} [(\delta x)^2 + (\Delta E(x;as))^2]p(x;s)dx \\
&= \int_{-\infty}^{+\infty} p(a)[\mathrm{VAR}[x;as] + (\Delta E(x;as))^2]da \\
&= \int_{-\infty}^{+\infty} p(a)\mathrm{VAR}[x;as]da + \int_{-\infty}^{+\infty} p(a)E^2[x;as]da - E^2[x;s].
\end{aligned}$$

This is the average of the conditional variance $\mathrm{VAR}[x;as]$, plus a term involving $(\Delta E(x;as))^2 = (E[x;as] - E[x;s])^2$. In the large noise limit,

$$\int_{-\infty}^{+\infty} p(a)E^2[x;as]da - E^2[x;s] \to s^2\mathrm{VAR}(a).$$

We also know from the initial discussion that, with increasing noise,

$$\mathrm{VAR}[x;as] \to [\Delta^2/12 + \sigma^2]$$

regardless of the amplitude of the scaled signal, as. Therefore,

$$\mathrm{VAR}[x;s] \to [\Delta^2/12 + \sigma^2] + s^2\mathrm{VAR}(a).$$

We note the specific form of the pdf $p(a)$ is here irrelevant. We identify that the variance increases with s^2. This undesirable effect can be eliminated when we normalize before averaging.

C.2 Normalized average

The signal in question is now $x_{i,j}/a_i = Q(a_i s_j + n_{i,j})/a_i$. The output x is scaled $x \to x/a$, such that its mean and standard deviation are also scaled with $1/a$. To the random variable x/a corresponds a new pdf,

$$P(x/a;s) = \int_{-\infty}^{+\infty} p(a)[ap(ax;as)]da,$$

where $ap(ax;as)$ is the conditional pdf of the scaled output (conditional on a), and p is the conditional pdf of the *un-scaled* output defined in the previous section. In general (e.g. (7), Sect. 5-28), the scaled output has an expectation of $E[x/a] = E[x]/a$ and a variance $\mathrm{VAR}[x/a] = VAR[x]/a^2$, expressed in the expectation and variance of the unscaled output. We get

$$\begin{aligned} E[x/a;s] &= \int_{-\infty}^{+\infty} xP(x/a;s)dx = \int_{-\infty}^{+\infty} p(a)E[x/a;as]da, \\ E[x/a;as] &= \frac{E[x;as]}{a}. \end{aligned}$$

As the noise increases, $E[x/a;as] \to s$ such that $E[x/a;s] \to s$.

Now for the variance. With

$$x/a - E[x/a;s] = (x/a - E[x/a;as]) + (E[x/a;as] - E[x/a;s]) \equiv \delta(x/a) + \Delta E(x/a;as),$$

we obtain

$$\begin{aligned} \mathrm{VAR}[x/a;s] &= \int_{-\infty}^{+\infty} p(a)[\mathrm{VAR}[x/a;as] + (\Delta E(x/a;as))^2]da, \\ \Delta E(x/a;as) &= E[x/a;as] - E[x/a;s], \\ \mathrm{VAR}[x/a;as] &= \frac{\mathrm{VAR}[x;as]}{a^2}. \end{aligned}$$

Also in this case can we use integrals over known conditional variances and expectations with $p(a)$ as weight. We obtain for the term $\Delta E(x/a;as)$;

$$\begin{aligned} (\Delta E(x/a;as))^2 &= E^2[x/a;as] - 2E[x/a;as]E[x/a;s] + E^2[x/a;s] \\ &= E^2[x/a;as] - E^2[x/a;s] - 2\Delta E(x/a;as)E[x/a;s]. \end{aligned}$$

When integrating over $p(a)$, $\Delta E(x/a;as)$ fluctuates around zero and gives a relatively small integrated result, such that

$$\mathrm{VAR}[x/a;s] \simeq \int_{-\infty}^{+\infty} p(a)[E^2[x/a;as] + VAR[x/a;as]]da - E^2[x/a;s].$$

This approximate result is on the same form as for simple averaging, except that the integrand is scaled with $1/a^2$.

As the noise increases, $\Delta E(x/a;as) \to 0$, because $E[x/a;as] \to s$ and $E[x/a;s] \to s$, such that

$$\mathrm{VAR}[x/a;s] \to \int_{-\infty}^{+\infty} p(a)\mathrm{VAR}[x/a;as]da.$$

The quadratic term in s is now eliminated as desired, although for small scaling a, the conditional $\mathrm{VAR}[x/a;as]$ is amplified as compared to $\mathrm{VAR}[x;as]$. For large noise, we know that $\mathrm{VAR}[x/a;as] = \mathrm{VAR}[x;as]/a^2 \to (\Delta^2/12 + \sigma^2)/a^2$, regardless of the conditional argument, such that

$$\mathrm{VAR}[x/a;s] \to [\Delta^2/12 + \sigma^2] \int_{-\infty}^{+\infty} \frac{p(a)}{a^2}da.$$

We note the dependency on the specific form of $p(a)$ in this case.

D THE VARIANCE OF I AND Q

The variance of $\bar{I}_j$ is

$$\mathrm{VAR}[\bar{I}_j] = E[(\bar{I}_j - E[\bar{I}_j])^2] = E[([\delta\bar{x}_j \cos(\omega_0 t_j)] \oplus h_j)^2].$$

For discrete convolution it generally holds that

$$A_j \oplus B_j = \sum_k A_k B_{j-k},$$

where A is stochastic in our case. The expectation of the squared term $(A_j \oplus B_j)^2$ is then

$$E[(A_j \oplus B_j)^2] = \sum_k \sum_l E[A_k A_l] B_{j-k} B_{j-l}.$$

For zero (or less than the sampling interval) correlation length, $E[A_k A_l] = \delta_{kl}$, and

$$E[(A_j \oplus B_j)^2] = \sum_k E[A_k^2] B_{j-k}^2.$$

Thus, the variance can be written in terms of the variance of the averaged quantized signal before I-Q demodulation;

$$\mathrm{VAR}[\bar{I}_j] = [E[(\delta\bar{x}_j)^2] \cos^2(\omega_0 t_j)] \oplus h_j^2.$$

Since the samples of the ensemble average are uncorrelated, we have

$$E[(\delta\bar{x}_j)^2] = \begin{cases} \mathrm{VAR}[x_{i,j}; s_j]/N & \text{Simple averaging} \\ \mathrm{VAR}[x_{i,j}/a_i; s_j]/N & \text{Normalized averaging} \end{cases}$$

E AMPLITUDE AND PHASE DISTRIBUTIONS FOR GAUSSIAN AND SYMMETRICALLY DISTRIBUTED I AND Q

In this section we review the statistics of amplitude and phase for arbitrary I and Q obeying Gaussian statistics. The probability distributions apply at any given time-lag within the pulse.

E.1 Amplitude distributions

Let $A_0 \equiv \sqrt{(E[I_j])^2 + (E[Q_j])^2}$ be the amplitude corresponding to the expectation values (we have shown that $E[I_j] = I(s_j)$ and $E[Q_j] = Q(s_j)$ in the regime $\sigma/\Delta \gg 1$). The pdf of the amplitude $A_j = \sqrt{(I_j)^2 + (Q_j)^2}$ is then Rician ((7), page 498) for each time sample j,

$$p(A; A_0, \sigma_I^2) = A/\sigma_I^2 e^{-(A^2+A_0^2)/2\sigma_I^2} I_0(AA_0/\sigma_I^2), \tag{E.1}$$

where I_0 is the modified Bessel function of zero order, and $\sigma_I^2 = \mathrm{VAR}[I_j] = \mathrm{VAR}[Q_j]$. The first and second moments are

$$\begin{aligned} E[A] &= \sigma_I \sqrt{\frac{\pi}{2}} \exp[-A_0^2/4\sigma_I^2][(1 + A_0^2/\sigma_I^2) I_0(A_0^2/4\sigma_I^2) + A_0^2/2\sigma_I^2 I_1(A_0^2/4\sigma_I^2)], \\ E[A^2] &= A_0^2 + 2\sigma_I^2, \end{aligned}$$

where I_1 is the modified Bessel function of first order.

For $A_0 \gg \sigma_I$, the quantity $x = A_0^2/4\sigma_I^2$ is very large. Thus the asymptotic relations

$$\begin{aligned} I_0(A_0^2/4\sigma_I^2) &= I_0(x) \sim \frac{e^x}{\sqrt{2\pi x}}(1+\frac{1}{8x}), \\ I_1(A_0^2/4\sigma_I^2) &= I_1(x) \sim \frac{e^x}{\sqrt{2\pi x}}(1-\frac{3}{8x}), \end{aligned}$$

are valid. After some algebra we arrive at the following expressions for the expectation and variance of the amplitude:

$$\begin{aligned} E[A] &= A_0 + \frac{\sigma_I}{2A_0} + \mathcal{O}((\frac{\sigma_I}{A_0})^3), \\ \mathrm{VAR}[A] &= \sigma_I^2 + \mathcal{O}((\frac{\sigma_I}{A_0})^2). \end{aligned}$$

It can be shown, using the asymptotic relations above, that the amplitude pdf approaches a Gaussian with mean $A_0 + \frac{\sigma_I}{2A_0}$ and variance σ_I^2 as $x = A_0^2/4\sigma_I^2$ grows (see e.g. Figure E.1, left panel, bottom).

For $A_0 \ll \sigma_I$, the pdf has support mainly for small A, and the argument of I_0 and I_1 is very small. Thus $I_0(x)$ can be replaced by 1, $I_1(x)$ can be replaced by $x/2$ and e^{-x} can be replaced by $1-x$ to a reasonable approximation. Thus the expectation and variance of the amplitude are

$$\begin{aligned} E[A] &= \sigma_I\sqrt{\frac{\pi}{2}}(1 + A_0^2/4\sigma_I^2) + \mathcal{O}((\frac{A_0}{\sigma_I})^4), \\ \mathrm{VAR}[A] &\simeq (2-\pi/2)\sigma_I^2 + (1-\pi/8)A_0^2. \end{aligned}$$

In the case $A_0 \ll \sigma_I$ the amplitude pdf is approximately a Rayleigh distribution (Figure E.1, top left).

It is important to note that $E[A] > A_0$ in general due to the variance (due to noise) in I_j and Q_j. That is, the expected amplitude is larger than the amplitude A_0 of the I-Q demodulated signal s. The noise to signal ratio σ_A/A_0 for $A_0 = 1$ is plotted in Figure E.2 as function of the input signal to noise ratio A_0/σ_I. The dashed and dashdotted lines represent the asymptotics of σ_A/A_0 in the limits $A_0/\sigma_I \to 0^+$ and $A_0/\sigma_I \to \infty$. Note that the amplitude noise to signal ratio lies between the two asymptotics for all input signal to noise ratios.

E.2 Phase distributions

The pdf of the phase, $\phi = \mathrm{Arg}(I_j + iQ_j)$, is $p(\phi - E[\phi]; q)$, where (page 501 in (7) and page 167 in (4)),

$$p(\phi; q) = \frac{e^{-q}}{2\pi} + \frac{\sqrt{q}\cos(\phi)e^{-q\sin^2(\phi)}}{\sqrt{4\pi}}\left[1 + 2\mathrm{Erf}(\sqrt{2q}\cos(\phi))\right], \quad q = \frac{A_0^2}{2\sigma_I^2}, \tag{E.2}$$

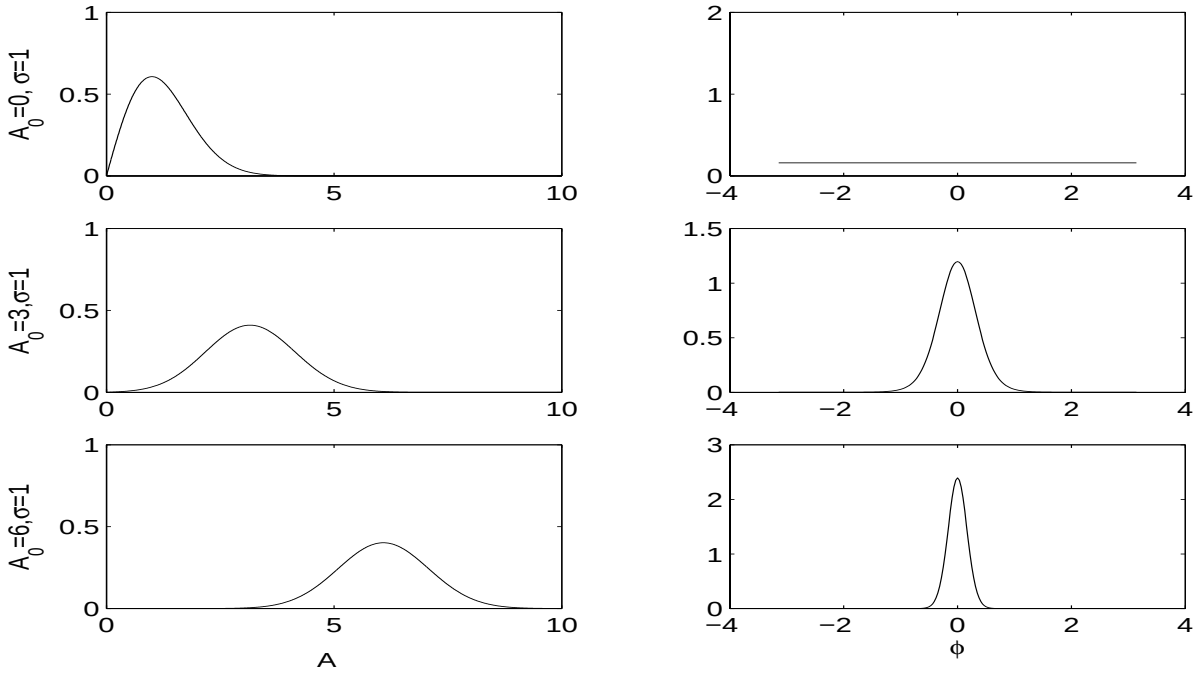

Figure E.1 *The amplitude pdf (left panel) and the phase pdf (right panel) for $A_0 = 0$, $\sigma_I = 1$ (top), $A_0 = 3$, $\sigma_I = 1$ (middle) and $A_0 = 6$, $\sigma_I = 1$ (bottom).*

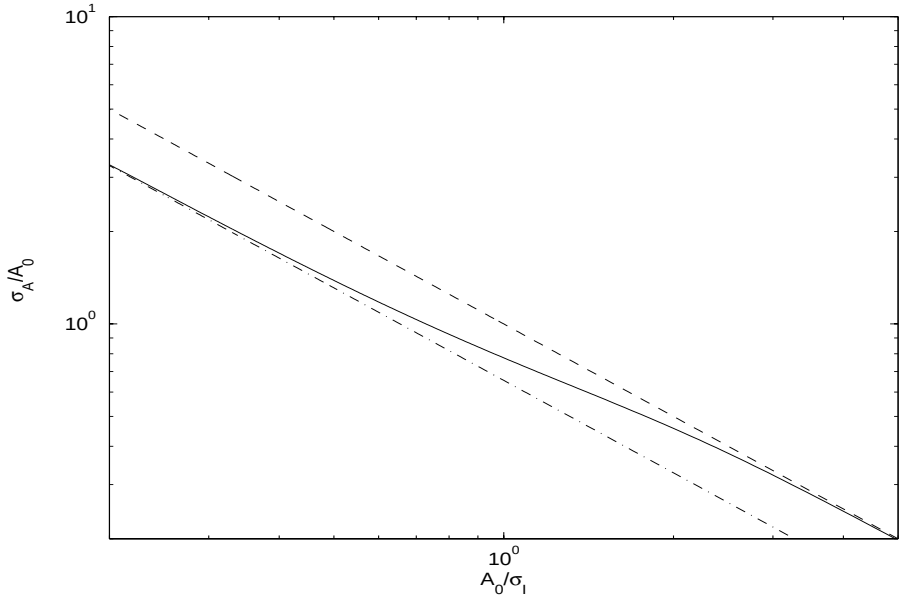

Figure E.2 *The relative standard deviation of the amplitude σ_A/A_0 when $A_0 = 1$ as a function of A_0/σ_I (solid line) and the asymptotics of the standard deviation in the limits $A_0/\sigma_I \to 0^+$ (dashdotted) and $A_0/\sigma_I \to \infty$ (dashed).*

and Erf denotes the usual error function; $\mathrm{Erf}(x) = (1/\sqrt{2\pi}) \int_0^x e^{-t^2/2}\, dt$. Due to symmetry properties in the complex plane, the expectation of the phase $E[\phi]$ is independent of A_0 and is equal to that of the input signal s:

$$E[\phi] = \mathrm{Arg}(E[I_j] + iE[Q_j]) = \mathrm{Arg}(I(s) + iQ(s)).$$

It is important to note that the variance of the phase, $\mathrm{VAR}[\phi]$, is dependent only on the square of the signal to noise ratio via $q = A_0^2/2\sigma_I^2$;

$$\mathrm{VAR}[\phi] = \int_{-\pi}^{\pi} (\phi - E[\phi])^2 p(\phi - E[\phi]; q)\, d\phi = \int_{-\pi+E[\phi]}^{\pi+E[\phi]} \phi^2 p(\phi; q)\, d\phi = \int_{-\pi}^{\pi} \phi^2 p(\phi; q)\, d\phi,$$

where the last equality is due to the periodicity of $p(\phi; q)$ with period 2π. In the rest of the section we consider, without loss of generality, the case $E[\phi] = 0$.

One can argue intuitively that the phase variance should be decreasing with increasing A_0: The concentration of the associated random numbers in the complex plane is further away from the origin for larger A_0 so the phase variance gets smaller (Figure E.1, right panels). Note that the pdf is uniform when the signal amplitude is zero (Figure E.1, right panel, top), as expected, and that the pdf approaches a Gaussian distribution with increasing A_0 (Figure E.1, right panel, middle and bottom). The Gaussian shape of the pdf can be explained by the following argument. When $q = A_0^2/(2\sigma_I^2) \gg 1$, the support of the pdf is mainly in the vicinity of $\phi = 0$, where the approximations $\sin^2 \phi \simeq \phi^2$ and $\cos \phi \simeq 1$ are accurate. Furthermore, the argument of the error function, $\sqrt{2q}\cos(\phi)$, is large so that $\mathrm{Erf}(\sqrt{2q}\cos(\phi)) \simeq \mathrm{Erf}(\sqrt{2q}) \simeq 1/2$. Thus we obtain the asymptotic expression

$$p(\phi; q) \sim 2\sqrt{\frac{q}{4\pi}} e^{-q\phi^2} = \frac{1}{\sqrt{2\pi}\sqrt{1/2q}} e^{-\frac{1}{2}(\frac{\phi}{\sqrt{1/2q}})^2}, \tag{E.3}$$

i.e. a Gaussian with mean zero and variance $1/2q = (\sigma_I/A_0)^2$.

In the opposite limit $q = A_0^2/(2\sigma_I^2) \ll 1$, the pdf is, approximately,

$$p(\phi; q) \sim \frac{1}{2\pi} + \sqrt{\frac{q}{4\pi}} \cos(\phi),$$

which has mean zero and variance $\pi^2/3 - 2\sqrt{q\pi}$. The phase standard deviation in degrees as function of the signal to noise ratio A_0/σ_I (solid line) and the asymptotics of the standard deviation in the limits $q \to 0^+$ (dashdotted) and $q \to \infty$ (dashed) are depicted in Figure E.3. We note that the phase standard deviation lies below the asymptotic in the limit $q \to \infty$ (dashed) for small values of A_0/σ_I, crosses this asymptotic and later converges to this asymptotic as q increases. Interestingly, σ_ϕ decreases very slowly for relatively low signal to noise ratios A_0/σ_I. When A_0/σ_I increases beyond 3, the decrease of σ_ϕ picks up speed.

E.3 Comments in relation to Method I

If we consider both variances to be functions of A_0/σ_I, the ensemble averaging represents compression of the A_0/σ_I-axis, according to $\sqrt{N}A_0/\sigma_I$. In other words, the variance function in terms of A_0/σ_I is forced in the direction of the vertical axis given by $A_0/\sigma_I = 0$. The amplitude

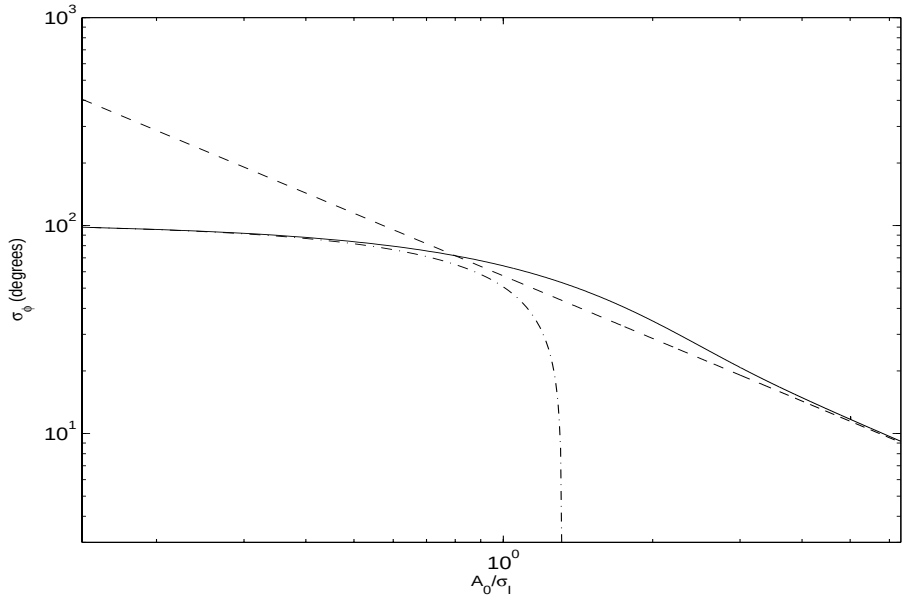

Figure E.3 The standard deviation of the phase σ_ϕ (in degrees) as a function of A_0/σ_I (solid line) and the asymptotics of the standard deviation in the limits $q = A_0^2/2\sigma_I^2 \to 0^+$ (dashdotted) and $q = A_0^2/2\sigma_I^2 \to \infty$ (dashed).

and phase variances as functions of A_0/σ_I are strictly decreasing, and this implies that the variances are also decreasing with increasing N. Consider the solid curves in Figures E.2 and E.3 representing amplitude and phase standard deviations for $N = 1$. Using Method I, the corresponding curves for $N > 1$ are obtained by contraction of the A_0/σ_I-axis using the transformation $A_0/\sigma_I \to \sqrt{N}A_0/\sigma_I$, i.e. forcing the curves in the direction of the vertical axis.

References

(1) Carbone P and Petri D (1994): Effect of Additive Dither on the Resolution of Ideal Quantizers. *IEEE Trans. Instrum. Meas.*, 43:389–396.

(2) DataRespons (2002): Dual Wideband Digital ESM-Receiver, Design and operation manual. Design and operation manual 39300-C01, DataRespons.

(3) DataRespons (2002): Dual Wideband Digital ESM-Receiver, Users manual. Users manual 39300-C02, DataRespons.

(4) Davenport W J and Root W (1958): *An Introduction to the Theory of Random Signals and Noise*.

(5) Eilevstjønn J (2001): FIA - programvare for klassifisering og identifikasjon av radarpulser. FFI/NOTAT 2001/02261, FFI (Ugradert).

(6) Øhra H, Smestad T and Malnes E (1999): Spesifikasjon av digitalt kanalkort til en avansert ESM-mottaker. FFI/RAPPORT 99/05264, FFI (Begrenset).

(7) Papoulis A (1965): *Probability, Random Variables, and Stochastic Processes*.

(8) Skartlien R (2003): Emitteridentifikasjon - effekter av flerveisutbredelse i radarpulser. FFI/NOTAT 2003/02842, FFI (Ugradert).

(9) Skartlien R and Øyehaug L (2003): Quantization error and resolution in ensemble averaged data with noise. Submitted to IEEE Trans. Instrum. Meas.

(10) Skartlien R, Sundgot R and Øyehaug L (2003): Metoder for pulssortering og emittergjenkjenning i ESMEX. FFI/RAPPORT 2003/00881, FFI (Ugradert).

(11) Sundgot R and Øyehaug L (2002): Metoder for emitteridentifisering i en ESM-demonstrator. FFI/RAPPORT 2002/00555, FFI (Ugradert).